Electronic Supplementary Material (ESI) for Chemical Science.
This journal is © The Royal Society of Chemistry 2015

Taming the Beast: Fluoromesityl Groups Induce a Dramatic Stability Enhancement in Boroles

Supporting Information

Zuolun Zhang,[a,b] Robert M. Edkins,[b] Martin Haehnel,[b] Marius Wehner,[b] Antonius Eichhorn,[b] Lisa Mailänder,[b] Michael Meier,[b] Johannes Brand,[b] Franziska Brede,[b] Klaus Müller-Buschbaum,[b] Holger Braunschweig,[b] and Todd B. Marder*[b]

[a] State Key Laboratory of Supramolecular Structure and Materials, College of Chemistry, Jilin University, Changchun 130012, P. R. China

[b] Institut für Anorganische Chemie, Julius-Maximilians-Universität Würzburg, Am Hubland, 97074 Würzburg, Germany

E-mail: todd.marder@uni-wuerzburg.de

Contents

Experimental section S3–S6

NMR, MS and single-crystal X-ray diffraction analyses of the mixture of Li[FMesBF_3], $LiBF_4$ and Et_2O (1:1.5:0.8) S7–S11

Single-crystal X-ray diffraction studies of **1** and **2** S12

DFT and TD-DFT calculations S13–S14

NMR spectra of **1**, **2** and **5** S15–S20

NMR and GC-MS analyses of the hydrolysis process of MesBC_4Ph_4, **1** and **2** in wet CD_2Cl_2 and in air; single-crystal X-ray diffraction of hydrolysed **2** S21–S29

Thermal analysis of **1** and **2** S30–S31

GC-MS of **1** and **2** S32–S33

NMR spectra showing the reversible binding of **1** and **2** with pyridine S34

References S35

Cartesian coordinates of all DFT-optimised structures S36–S38

Experimental section

General information

1,3,5-Tris(trifluoromethyl)benzene (FMesH),[1] 1,4-diiodo-1,2,3,4-tetraphenylbuta-1,3-diene,[2] 1,2-bis(iodo(phenyl)methylene)cyclopentane[3] and 1-mesityl-2,3,4,5-tetraphenylborole[4] were prepared according to literature procedures. All other starting materials were purchased from commercial sources and were used without further purification. The organic solvents for synthetic reactions and for photophysical and electrochemical measurements were HPLC grade, further treated to remove trace water using an Innovative Technology Inc. Pure-Solv Solvent Purification System and deoxygenated using the freeze-pump-thaw method. All synthetic reactions were performed in an Innovative Technology Inc. glovebox or under an argon atmosphere using standard Schlenk techniques. ^{1}H, ^{13}C{^{1}H}, ^{19}F, ^{19}F{^{1}H}, ^{11}B and ^{7}Li NMR spectra were measured either on a Bruker Avance 500 (^{1}H, 500 MHz; ^{13}C{^{1}H}, 125 MHz; ^{19}F, 470 MHz; ^{11}B, 160 MHz; ^{7}Li, 194 MHz) or on a Bruker Avance 200 (^{1}H, 200 MHz; ^{19}F{^{1}H}, 188 MHz) NMR spectrometer. Mass spectra were recorded on Agilent 7890A/5975C Inert GC/MSD systems operating in EI mode. Elemental analyses were performed on a Leco CHNS-932 Elemental Analyser. UV–visible–NIR absorption spectra were recorded in standard quartz cuvettes (1 cm x 1 cm cross-section) using a Varian Cary 5E UV-visible spectrophotometer. All solutions used in photophysical measurements had concentrations lower than 5×10^{-5} M. Thermogravimetric analysis (TGA) was performed on a NETZSCH STA-409 thermogravimetric analyser at a heating rate of 10 °C min^{-1} under a constant gas flow of an argon/nitrogen mixture (40 mL min^{-1}). Differential scanning calorimetry (DSC) measurements were conducted on a Mettler Toledo DSC 823 at a heating rate of 10 °C min^{-1} under a constant gas flow of nitrogen.

Single-crystal X-ray diffraction

Crystals suitable for single-crystal X-ray diffraction were selected, coated in perfluoropolyether oil, and mounted on MiTeGen sample holders. The crystal data for **1**, **2**, hydrolysed **2**, and the Li[FMesBF$_3$]-containing co-crystal were collected on a Bruker X8-APEX II diffractometer with a CCD area detector and multi-layer mirror monochromated Mo Kα radiation. The structures were solved using the intrinsic phasing method (ShelXT), refined with the ShelXL program[5] and expanded using Fourier techniques. All non-hydrogen atoms were refined anisotropically. Hydrogen atoms were included in structure factor calculations. All hydrogen atoms were assigned to idealised geometric positions. The crystal of hydrolysed **2** was a pseudo-merohedral twin with domains rotated by 180° around real axis [0.054 0.000 1.000]. The BASF parameter was refined to 37%.

Electrochemical measurements

All cyclic voltammetry experiments were conducted in an argon-filled glovebox using a Gamry Instruments Reference 600 potentiostat. A standard three-electrode cell configuration was employed using a platinum disk working electrode, a platinum wire counter electrode, and a silver wire reference electrode separated by a Vycor frit. Compensation for resistive losses (*IR* drop) was employed for all measurements. A 0.1 M solution of $[NBu_4][PF_6]$ was used as the supporting electrolyte. A scan rate of 150 mV s^{-1} was used.

Theoretical studies

All calculations were carried out with the program package Gaussian 09 (Revision D.01).[6] GaussView 5.0 was used to visualise the results, to measure calculated distances and bond lengths, and to plot orbital surfaces. The molecular structures of **1**, **2** and $MesBC_4Ph_4$[4] as determined by X-ray crystallography were used as the input for optimising their ground-state geometries. A second starting geometry of **2** was considered, in which the phenyl groups in the 2- and 5-positions were in an *anti*-configuration relative to the borole plane, rather than the *syn*-conformation found in the crystal structure; however, the located minimum was marginally higher in energy than the first (+0.3 kcal mol^{-1}) and was not considered further. The ground-state geometries were optimised using the PBE0 functional[7] in combination with the 6-31+G(d,p)[8] basis set. This level of theory was chosen to allow comparison of our results with those reported by Braunschweig and co-workers for related boroles, which were obtained from calculations performed using the same method.[9] The ultrafine integration grid implemented in Gaussian 09 was used in optimization calculations. The optimised geometries were confirmed to be local minima by performing frequency calculations and obtaining only positive (real) frequencies. The stability of the wavefunction was also confirmed in each case. Based on these optimised structures, the lowest energy gas-phase vertical transitions were calculated (singlets, 25 states) by TD-DFT using the CAM-B3LYP[10] functional in combination with the 6-31+G(d,p) basis set. Symmetry constraints were not used in any of the calculations. GaussSum[11] was used to simulate the absorption spectra using Gaussian curves of 4800 cm^{-1} full width at half maximum (fwhm); this value was taken from the experimental bandwidth of the low-energy band of **1**. The nucleus-independent chemical shift (NICS) at the geometric centre of the borole (*i.e.* the NICS(0) value) was obtained by taking the negative of the isotropic NMR chemical shift of a ghost atom placed at this point calculated using the gauge-independent atomic orbital (GIAO) method. NICS calculations were performed at the optimised geometry using the PBE0/6-31+G(d,p) level of theory; the default fine integration grid was used. Use of the ultrafine integration grid gave larger values that were not comparable with those reported previously.[9] In general, a positive NICS(0) value is obtained for an antiaromatic ring, while for an aromatic ring it is negative. Note: comparing the NICS(0) values of two boroles at their respective optimised geometries does not differentiate between geometric (*e.g.* changes in dihedral angles due to steric hindrance) and electronic effects of changing the substituent.

Synthesis

Lithium trifluoro(fluoromesityl)borate (Li[FMesBF$_3$]). *n*-BuLi (1.6 M in hexane, 11.0 mL, 18 mmol) was slowly added to a solution of 1,3,5-tris(trifluoromethyl)benzene (5.00 g, 17.7 mmol) in Et$_2$O (9 mL) at –78 °C and then the mixture was slowly warmed to r.t. over 3 h. After stirring at r.t. for 1 h, the mixture was added slowly to a solution of BF$_3$•OEt$_2$ (1.58 mL, 12.8 mmol) in Et$_2$O (28 mL) at –78 °C. The reaction mixture was slowly warmed to 0 °C and then stirred at r.t. overnight. After removing the volatiles *in vacuo*, Et$_2$O (6 mL) and hexane (12 mL) were added sequentially to the residue to form a solution. By removing about half of the solvent, a solid precipitated. The solid was collected by filtration and then stirred in hexane (20 mL) for 20 min. Filtration gave the crude product as a white solid (1.70 g). NMR measurements indicated that the solid was a mixture of Li[FMesBF$_3$], LiBF$_4$ and Et$_2$O with a molar ratio of about 1.0:1.5:0.8. Because of the difficulty in further purification of the desired compound, the crude product was used directly in the syntheses of the boroles. ^{1}H NMR (500 MHz, THF-*d*$_8$, r.t., ppm): *δ* 8.04 (s). ^{13}C{^{1}H} NMR (125 MHz, THF-*d*$_8$, r.t., ppm): *δ* 153.3 (br.), 137.8 (q, $^2J_{\text{C–F}}$ = 32 Hz), 129.2 (q, $^2J_{\text{C–F}}$ = 33 Hz), 126.0 (br.), 125.4 (q, $^1J_{\text{C–F}}$ = 275 Hz), 124.7 (q, $^1J_{\text{C–F}}$ = 272 Hz). ^{19}F NMR (470 MHz, THF-*d*$_8$, r.t., ppm): *δ* –58.4 (q, $J_{\text{F–F}}$ = 14 Hz, 6 F), –63.8 (s, 3 F), –139.8 (m, br, 3 F). ^{11}B NMR (160 MHz, THF-*d*$_8$, r.t., ppm): *δ* 2.2 (q, $^1J_{\text{B–F}}$ = 43 Hz). MS (EI$^+$) *m/z*: 356 [M]$^+$, 337 [M–F]$^+$, 311 [M–2F–Li]$^+$.

1-Fluoromesityl-2,3,4,5-tetraphenylborole (1). *t*-BuLi (1.7 M in pentane, 3.62 mL, 6.2 mmol) was added to a suspension of 1,4-diiodo-1,2,3,4-tetraphenylbuta-1,3-diene (940 mg, 1.54 mmol) in Et$_2$O (23 mL) at –78 °C. The mixture was slowly warmed to –35 °C during the course of 1 h and then the solvent was evaporated *in vacuo* to leave a solid residue, to which hexane (10 mL) was added and the mixture was stirred for 10 min at r.t. and then filtered. The obtained solid, toluene (38 mL), and the as-prepared Li[FMesBF$_3$]-containing mixture (738 mg, containing *ca*. 473 mg, 1.33 mmol Li[FMesBF$_3$]) were added to a flask and stirred overnight. After removing the solvent *in vacuo*, hexane (70 mL) was added to the residue, and the resulting mixture was stirred for 30 min and then filtered. The obtained filtrate was concentrated, heated to reflux and then cooled to 0 °C to produce the desired compound as black crystals (525 mg, 53% based on 1,4-diiodo-1,2,3,4-tetraphenylbuta-1,3-diene). Single crystals for X-ray diffraction were obtained by slow evaporation of a diethyl ether/hexane mixed-solvent solution of **1** at r.t. ^{1}H NMR (500 MHz, CD$_2$Cl$_2$, r.t., ppm): *δ* 8.04 (s, 2 H), 7.19–7.16 (m, 2 H), 7.11–7.08 (m, 4 H), 7.00–6.96 (m, 6 H), 6.87–6.85 (m, 4 H), 6.72–6.70 (m, 4 H). ^{13}C{^{1}H} NMR (125 MHz, CD$_2$Cl$_2$, r.t., ppm): *δ* 163.1, 142.3 (br.), 138.5 (br.), 137.8, 136.1, 132.5 (q, $^2J_{\text{C–F}}$ = 33 Hz), 132.1 (q, $^2J_{\text{C–F}}$ = 35 Hz), 129.8, 128.9, 128.2, 128.1, 127.9, 126.9 (br.), 126.4, 124.3 (q, $^1J_{\text{C–F}}$ = 275 Hz), 123.1 (q, $^1J_{\text{C–F}}$ = 273 Hz). ^{19}F{^{1}H} NMR (188 MHz, CD$_2$Cl$_2$, r.t., ppm): *δ* –59.8 (s, 6 F), –63.5 (s, 3 F). ^{11}B NMR (160 MHz, CD$_2$Cl$_2$, r.t., ppm): *δ* 72 (br.). MS (EI$^+$) *m/z*: 648 [M]$^+$. Elem. Anal. Calcd (%) for $C_{37}H_{22}BF_9$: C, 68.54; H, 3.42. Found: C, 68.74; H, 3.42.

1-Fluoromesityl-2,5-diphenyl-3,4-(μ-(CH_2)$_3$)borole (2). *t*-BuLi (1.7 M in pentane, 2.37 mL, 4.0 mmol) was added to a suspension of 1,2-bis(iodo(phenyl)methylene)cyclopentane (500 mg, 1.0 mmol) in Et_2O (15 mL) at –78 °C. The mixture was slowly warmed to –30 °C during the course of 1 h and then the solvent was evaporated *in vacuo* to leave a solid residue, to which hexane (8 mL) was added and the mixture was stirred for 10 min at r.t. and then filtered. The obtained solid, toluene (25 mL), and the as-prepared Li[$FMesBF_3$]-containing mixture (479 mg, containing *ca.* 306 mg, 0.86 mmol Li[$FMesBF_3$]) were added to a flask and stirred overnight. After removing the solvent *in vacuo*, hexane (40 mL) was added to the residue, and the resulting mixture was stirred for 30 min and then filtered. The obtained filtrate was concentrated to *ca.* 5 mL, and then Et_2O (10 mL) was added to give a clear solution. Slow solvent evaporation produced the crude product, which was heated at 110 °C (1.5 h) under vacuum (100 mTorr) to remove a small amount of volatile impurities. The pure product was isolated as black crystals (223 mg, 42% based on 1,2-bis(iodo(phenyl)methylene)cyclopentane). ^{1}H NMR (500 MHz, CD_2Cl_2, r.t., ppm): δ 8.15 (s, 2 H), 7.16–7.13 (m, 4 H), 7.08–7.05 (m, 2 H), 6.94–6.93 (m, 4 H), 2.72 (t, J = 7 Hz, 4 H), 2.20 (quintet, J = 7 Hz, 2 H). ^{13}C{^{1}H} NMR (125 MHz, CD_2Cl_2, r.t., ppm): δ 172.5, 143.9 (br.), 137.7, 132.1 (q, $^2J_{C–F}$ = 35 Hz), 132.0 (q, $^2J_{C–F}$ = 34 Hz), 129.6 (br.), 128.6, 127.2, 127.1 (br.), 126.2, 124.3 (q, $^1J_{C–F}$ = 275 Hz), 123.2 (q, $^1J_{C–F}$ = 273 Hz), 28.8, 27.9. ^{19}F{^{1}H} NMR (188 MHz, CD_2Cl_2, r.t., ppm): δ –60.2 (s, 6 F), –63.4 (s, 3 F). ^{11}B NMR (160 MHz, CD_2Cl_2, r.t., ppm): δ 72 (br.). MS (EI$^+$) *m/z*: 536 [M]$^+$. Elem. Anal. Calcd (%) for $C_{28}H_{18}BF_9$: C, 62.71; H, 3.38. Found: C, 63.07; H, 3.32.

Isomerization of 2 under strongly basic conditions to 5. Compound **2** (22 mg, 0.041 mmol), THF (2 mL) and NaOH (4.0 mg, 0.1 mmol) were added sequentially to a sample vial, and then the mixture was stirred overnight at r.t. All of the volatiles were removed *in vacuo*, and the residue was purified by column chromatography (neutral Al_2O_3, hexane) to produce compound **5** as a white solid (17 mg, 77%). ^{1}H NMR (500 MHz, THF-d_8, r.t., ppm): δ 8.36 (s, 1 H), 8.03 (s, 1 H), 7.14–7.11 (m, 4 H), 7.05–7.01 (m, 3 H), 6.97–6.94 (m, 1 H), 6.85–6.83 (m, 2 H), 6.31 (m, 1 H), 3.79 (s, 1 H), 3.22–3.14 (m, 2 H), 3.09–3.02 (m, 2 H). ^{13}C{^{1}H} NMR (125 MHz, THF-d_8, r.t., ppm): δ 193.2, 157.7, 144.4 (br.), 139.6, 139.5 (br.), 139.3, 135.2, 133.7 (q, $^2J_{C–F}$ = 33 Hz), 132.6 (q, $^2J_{C–F}$ = 32 Hz), 132.0 (q, $^2J_{C–F}$ = 34 Hz), 128.9, 128.7, 128.3, 128.0, 127.5 (br.), 127.2 (br.), 126.8, 125.8, 125.1 (q, $^1J_{C–F}$ = 275 Hz), 124.1 (q, $^1J_{C–F}$ = 275 Hz), 124.0 (q, $^1J_{C–F}$ = 272 Hz), 45.8 (br.), 37.8, 28.7. ^{19}F NMR (470 MHz, THF-d_8, r.t., ppm): δ –57.9 (s, 3 F), –58.9 (s, 3 F), –63.8 (s, 3 F). ^{11}B NMR (160 MHz, THF-d_8, r.t., ppm): δ 73 (br.). MS (EI$^+$) *m/z*: 536 [M]$^+$.

NMR, MS and single-crystal X-ray diffraction analyses of the mixture of Li[FMesBF_3], $LiBF_4$ and Et_2O (1:1.5:0.8)

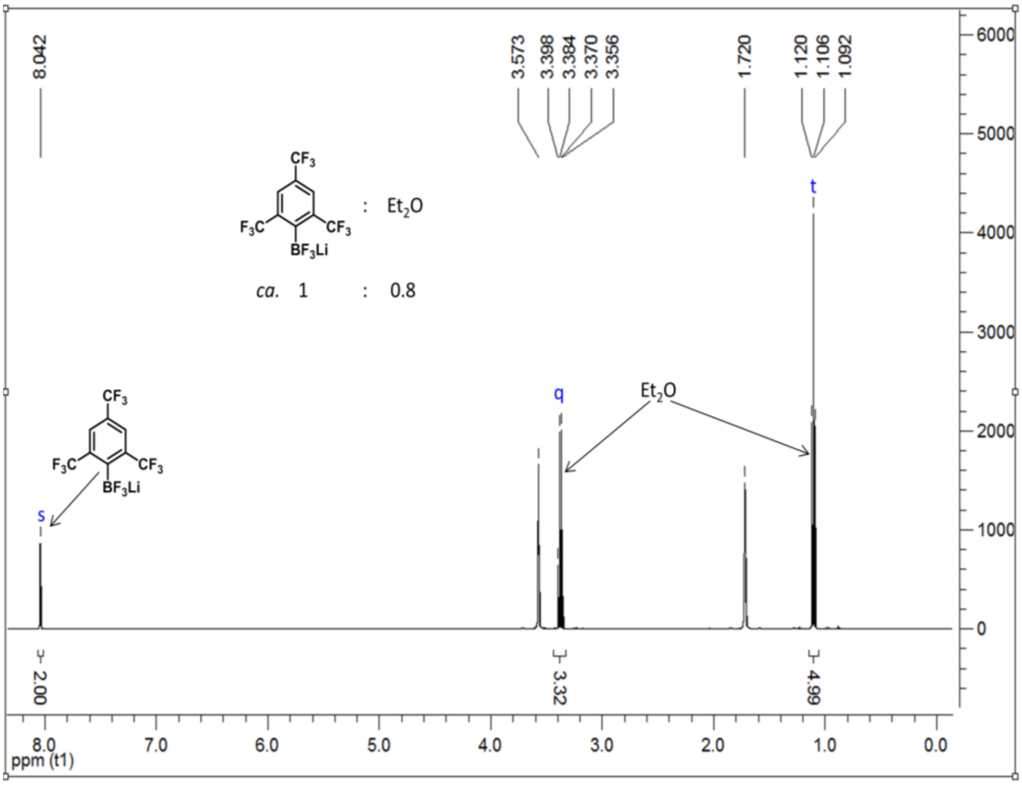

Fig. S1 ^{1}H NMR spectrum of the mixture of Li[FMesBF_3], $LiBF_4$ and Et_2O with a molar ratio of *ca.* 1:1.5:0.8 measured in THF-d_8 at 500 MHz.

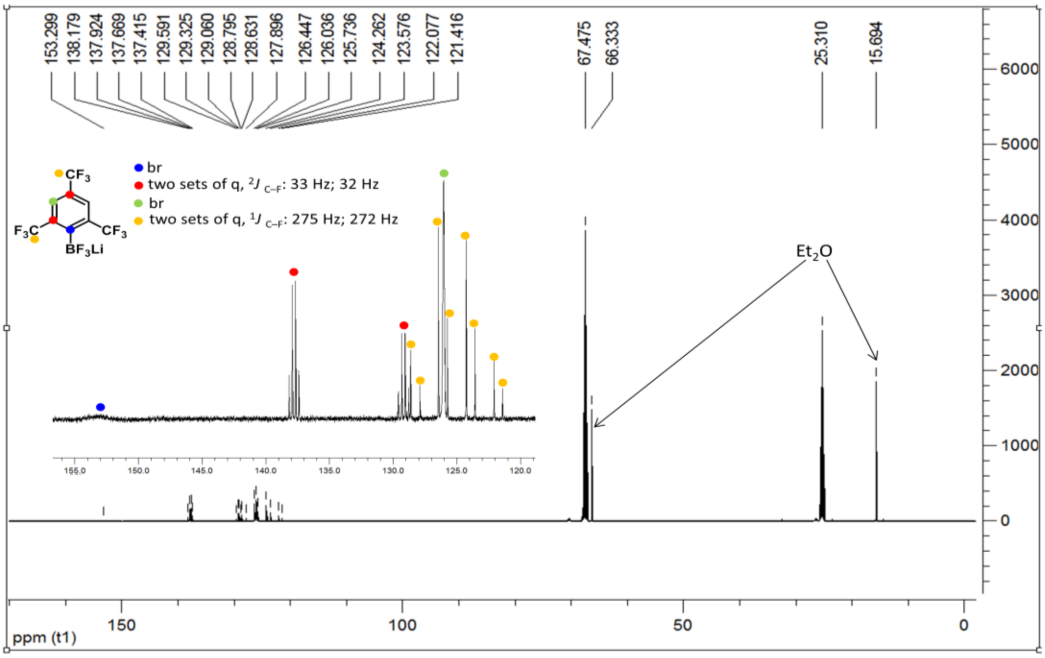

Fig. S2 ^{13}C{^{1}H} NMR spectrum of the mixture of Li[FMesBF_3], $LiBF_4$ and Et_2O with a molar ratio of *ca.* 1:1.5:0.8 measured in THF-d_8 at 125 MHz.

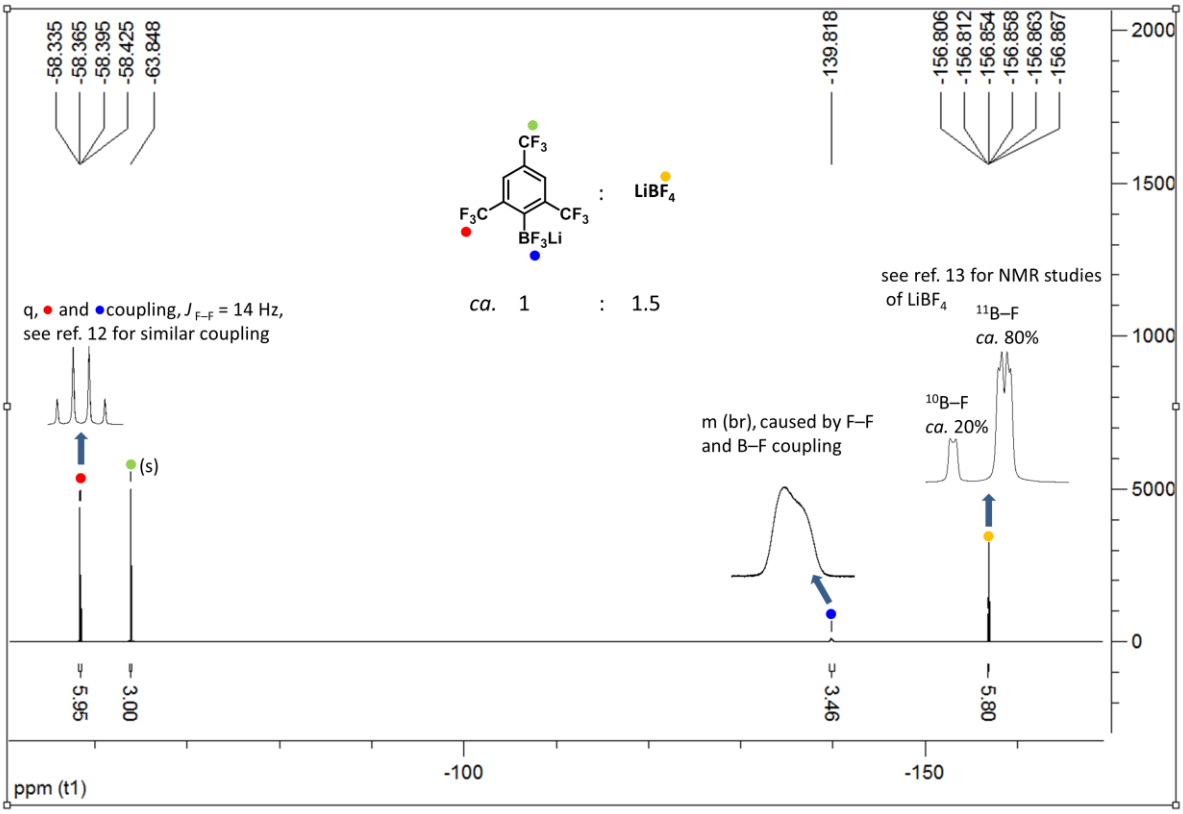

Fig. S3 ^{19}F NMR spectrum of the mixture of Li[FMesBF$_3$], LiBF$_4$ and Et$_2$O with a molar ratio of *ca.* 1:1.5:0.8 measured in THF-d_8 at 470 MHz.

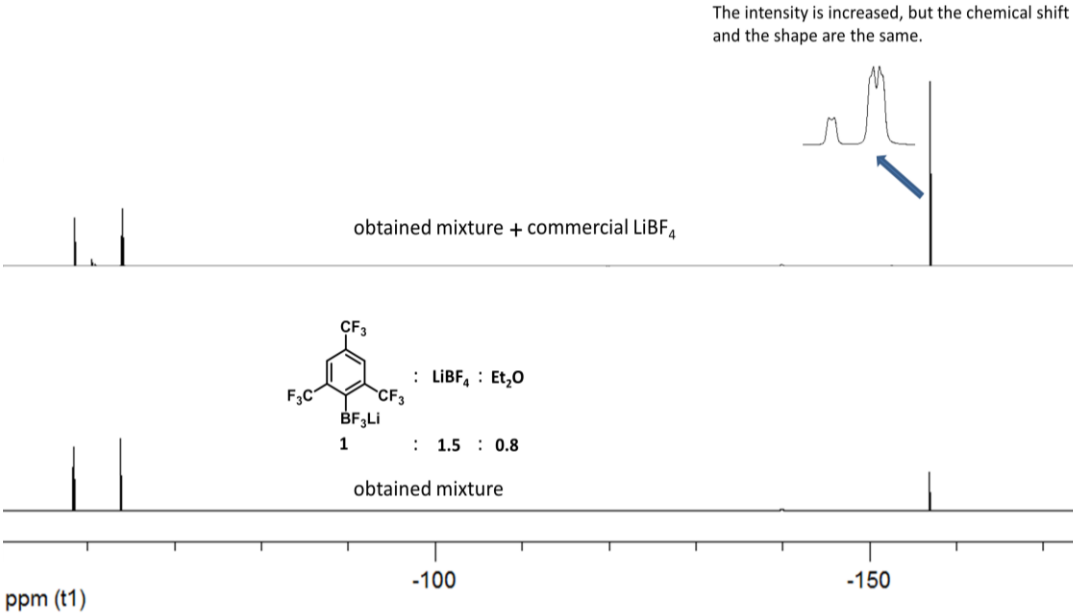

Fig. S4 ^{19}F NMR spectra confirming the existence of LiBF$_4$ in the obtained mixture measured in THF-d_8 at 470 MHz.

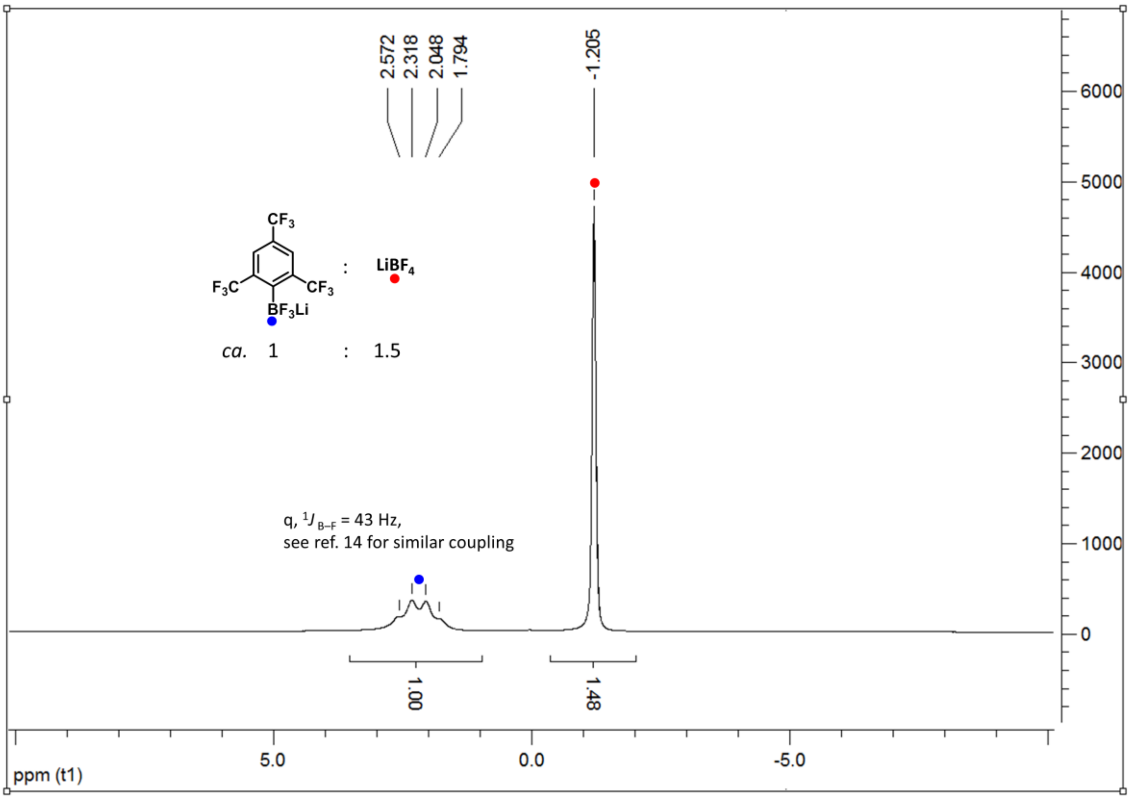

Fig. S5 ^{11}B NMR spectrum of the mixture of Li[FMesBF$_3$], LiBF$_4$ and Et$_2$O with a molar ratio of *ca.* 1:1.5:0.8 measured in THF-d_8 at 160 MHz.

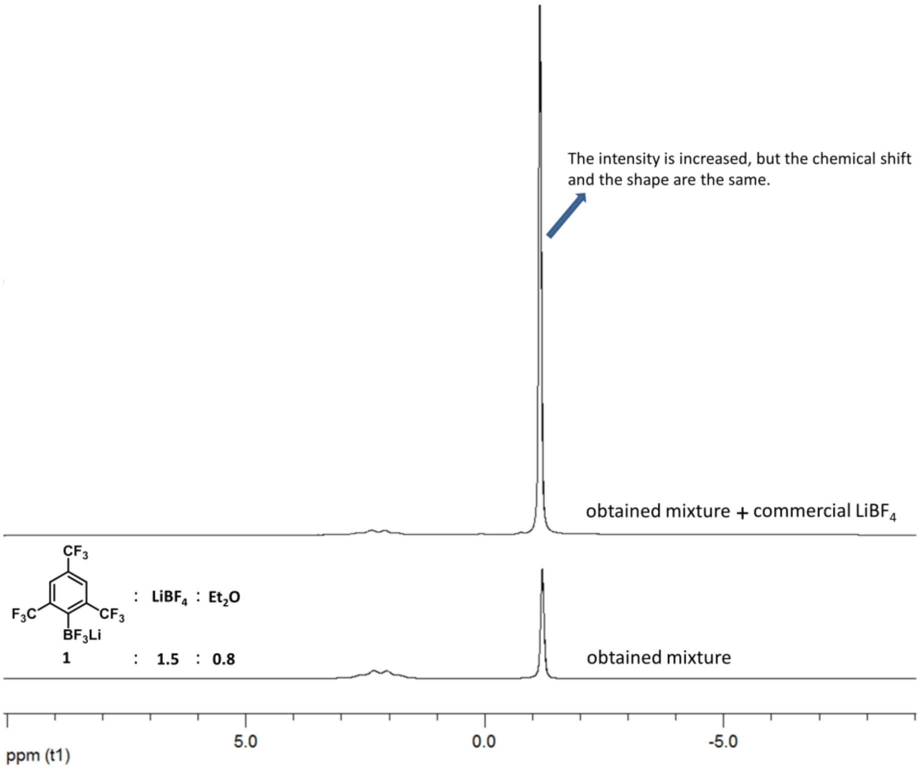

Fig. S6 ^{11}B NMR spectra confirming the existence of LiBF$_4$ in the obtained mixture measured in THF-d_8 at 160 MHz.

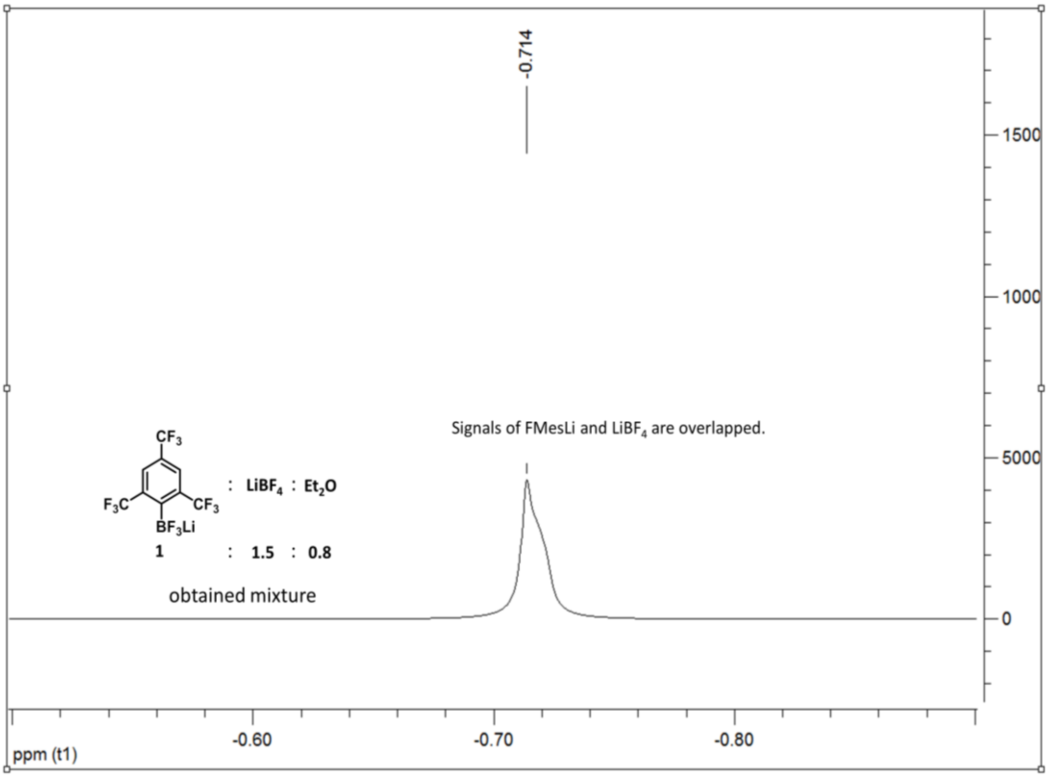

Fig. S7 ^{7}Li NMR spectrum of the mixture of Li[FMesBF$_3$], LiBF$_4$ and Et$_2$O with a molar ratio of *ca.* 1:1.5:0.8 measured in THF-d_8 at 194 MHz.

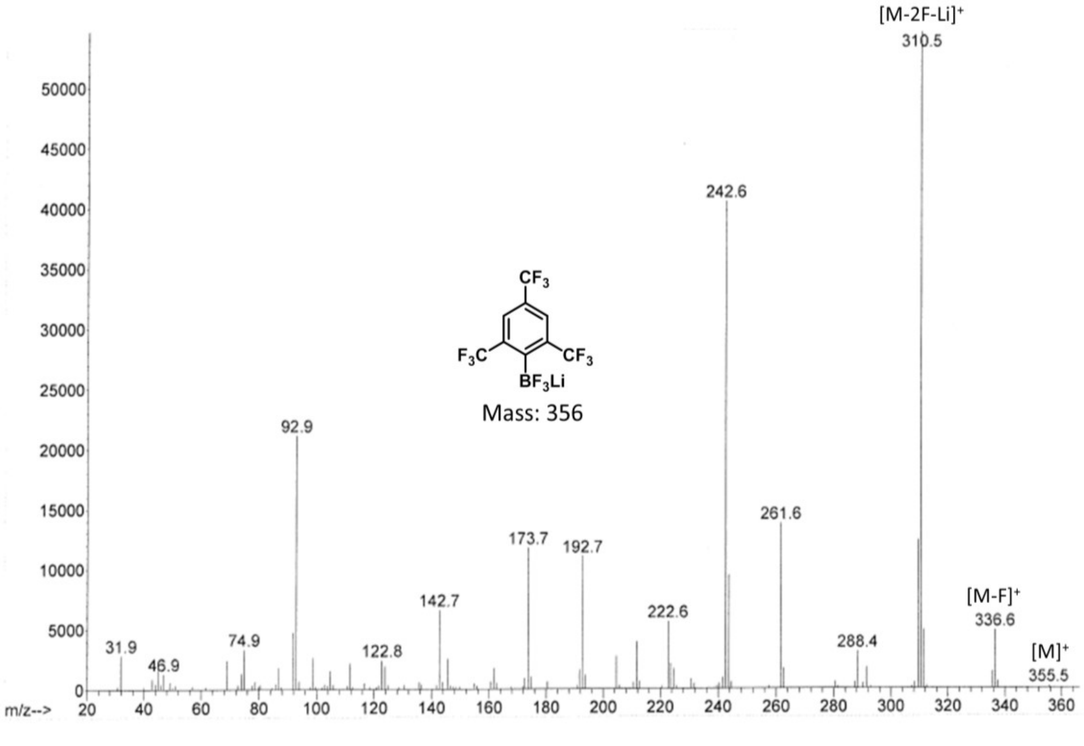

Fig. S8 EI^{+} mass spectrum of Li[FMesBF$_3$].

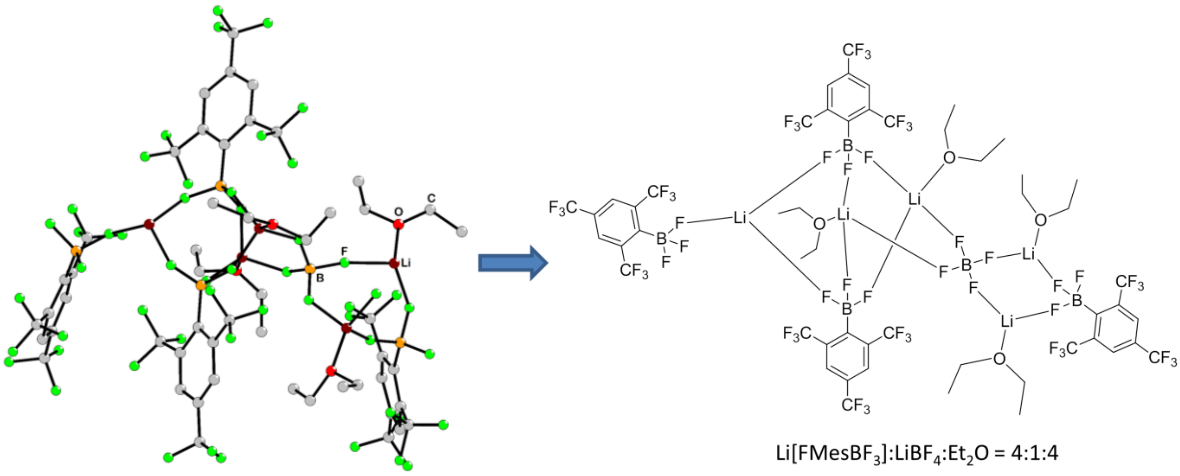

Fig. S9 The structure in the asymmetric unit of the single crystal obtained by slow solvent evaporation of the solution (in Et_2O/hexane mixed solvent) of the mixture of Li[FMesBF_3], $LiBF_4$ and Et_2O (*ca.* 1:1.5:0.8). Atom colour code: carbon (grey), fluorine (green), boron (orange), oxygen (red). Hydrogen atoms have been omitted for clarity. The quality of the crystal data is poor. However, the existence of Li[FMesBF_3] and $LiBF_4$ in the obtained mixture can be clearly confirmed by this crystal structure.

Crystal Data: $C_{52}H_{48}B_5F_{52}Li_5O_4$, $M_r = 1813.65$, Bruker APEX-II CCD, monoclinic, $P2_1/c$, $a = 13.166(4)$ Å, $b = 24.396(8)$ Å, $c = 24.064(8)$ Å, $\beta = 99.894(12)°$, $V = 7614(4)$ Å^3, $Z = 4$, $\rho_{\text{calcd}} = 1.582$ g cm^{-3}, $\mu = 0.183$ mm^{-1}, $F(000) = 3600$, $T = 100(2)$ K, $R_1 = 0.1589$, $wR_2 = 0.2715$, 11941 independent reflections [$2\theta \leq 50°$] and 1113 parameters.

Single-crystal X-ray diffraction studies of 1 and 2

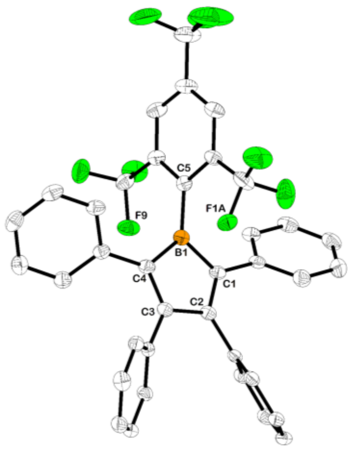

Fig. S10 The molecular structure of **1** as determined by X-ray crystallography. Atom colour code: carbon (grey), fluorine (green), boron (orange). Hydrogen atoms have been omitted for clarity. Atomic displacement ellipsoids are drawn at 50% probability.

Crystal Data: $C_{37}H_{22}BF_9$, $M_r = 648.35$, Bruker APEX-II CCD, triclinic, P-1, $a = 10.1241(4)$ Å, $b = 10.1353(4)$ Å, $c = 17.3058(6)$ Å, $\alpha = 84.1092(12)°$, $\beta = 73.8330(12)°$, $\gamma = 63.9157(11)°$, $V = 1531.42(10)$ Å^3, $Z = 2$, $\rho_{\text{calcd}} = 1.406$ g cm^{-3}, $\mu = 0.119$ mm^{-1}, $F(000) = 660$, $T = 100(2)$ K, $R_1 = 0.0620$, $wR_2 = 0.1337$, 5682 independent reflections [$2\theta \leq 51.0°$] and 452 parameters.

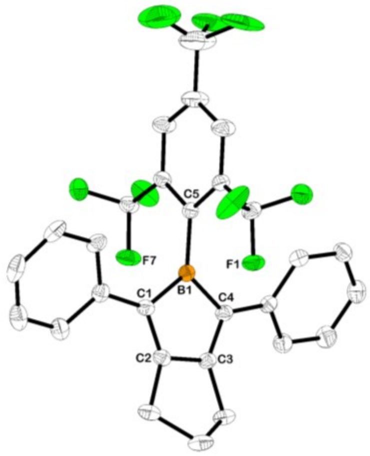

Fig. S11 The molecular structure of **2** as determined by X-ray crystallography. Atom colour code: carbon (grey), fluorine (green), boron (orange). Hydrogen atoms have been omitted for clarity. Only one of the two independent molecules in the asymmetric cell is shown. Atomic displacement ellipsoids are drawn at 50% probability.

Crystal Data: $C_{28}H_{18}BF_9$, $M_r = 536.23$, Bruker APEX-II CCD, triclinic, P-1, $a = 9.7736(5)$ Å, $b = 16.1049(8)$ Å, $c = 16.4046(8)$ Å, $\alpha = 76.766(2)°$, $\beta = 74.775(2)°$, $\gamma = 75.510(2)°$, $V = 2375.1(2)$ Å^3, $Z = 4$, $\rho_{\text{calcd}} = 1.500$ g cm^{-3}, $\mu = 0.135$ mm^{-1}, $F(000) = 1088$, $T = 100(2)$ K, $R_1 = 0.0485$, $wR_2 = 0.1103$, 8409 independent reflections [$2\theta \leq 50.1°$] and 740 parameters.

DFT and TD-DFT calculations

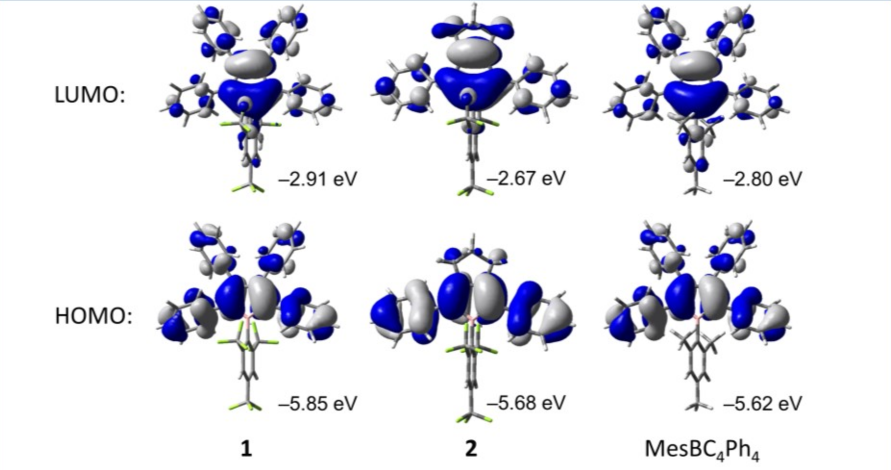

Compound	Transition (*f*)	*E* / eV	*λ* / nm	Dominant Components *a*
1	$S_1 \leftarrow S_0$ (0.021)	2.17	573	LUMO ← HOMO (94%)
2	$S_1 \leftarrow S_0$ (0.068)	2.23	558	LUMO ← HOMO (93%)
$MesBC_4Ph_4$	$S_1 \leftarrow S_0$ (0.019)	2.03	610	LUMO ← HOMO (95%)

a Components with greater than 10% contribution shown. Percentage contribution approximated by 2 x $(ci)^2$ x 100%, where *ci* is the coefficient for the particular orbital rotation.

Fig. S12 DFT (PBE0/6-31+G(d,p)) calculated frontier orbitals (surface isovalue: ±0.02 [*e* $a_0^{-3}]^{½}$) and orbital energies, as well as TD-DFT (CAM-B3LYP/6-31+G(d,p)//PBE0/6-31+G(d,p)) calculated photophysical data for **1**, **2** and $MesBC_4Ph_4$.

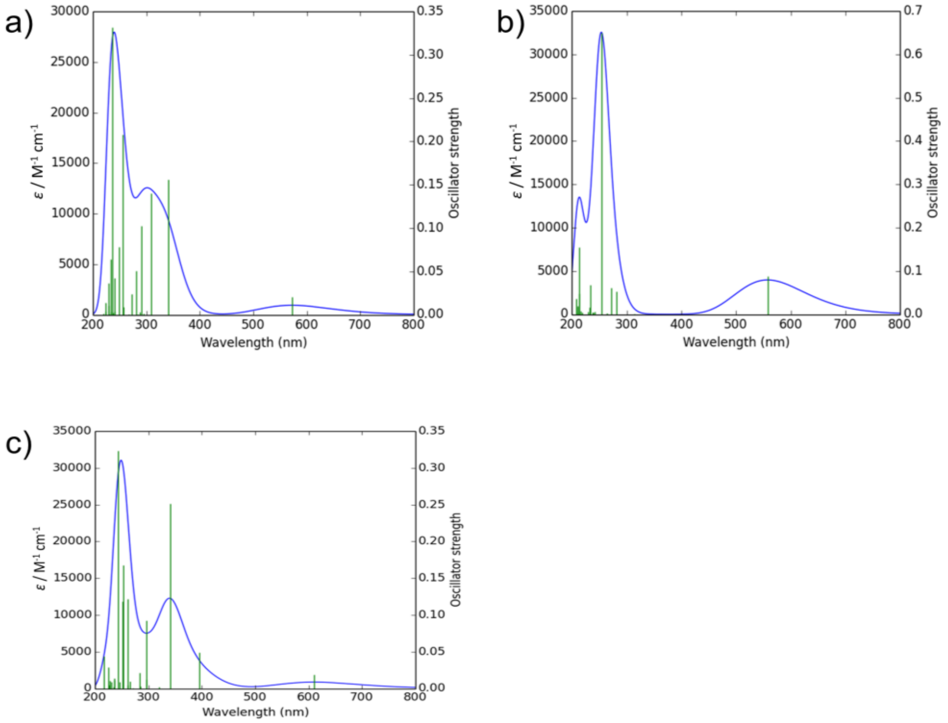

Fig. S13 Calculated absorption spectra of a) **1**, b) **2**, and c) $MesBC_4Ph_4$ at the CAM-B3LYP/6-31+G(d,p)//PBE0/6-31+G(d,p) level of theory with 25 singlet states and simulated with a Gaussian bandwidth of 4800 cm^{-1} fwhm (obtained from the experimental bandwidth of the low energy band).

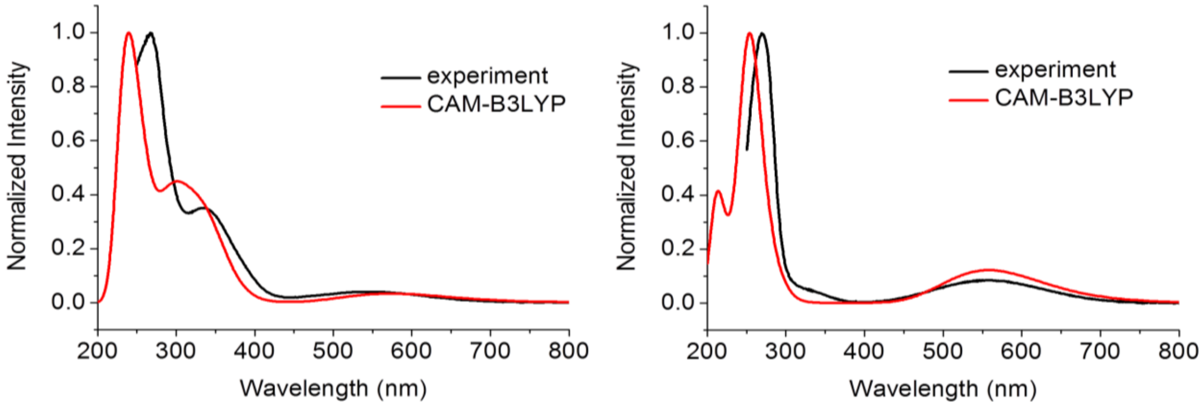

Fig. S14 Comparison of calculated and experimental absorption spectra of (left) **1** and (right) **2**. Calculated at the CAM-B3LYP/6-31+G(d,p)//PBE0/6-31+G(d,p) level of theory with 25 singlet states and simulated with a Gaussian bandwidth of 4800 cm^{-1} fwhm (obtained from the experimental bandwidth of the low energy band).

NMR spectra of 1, 2 and 5

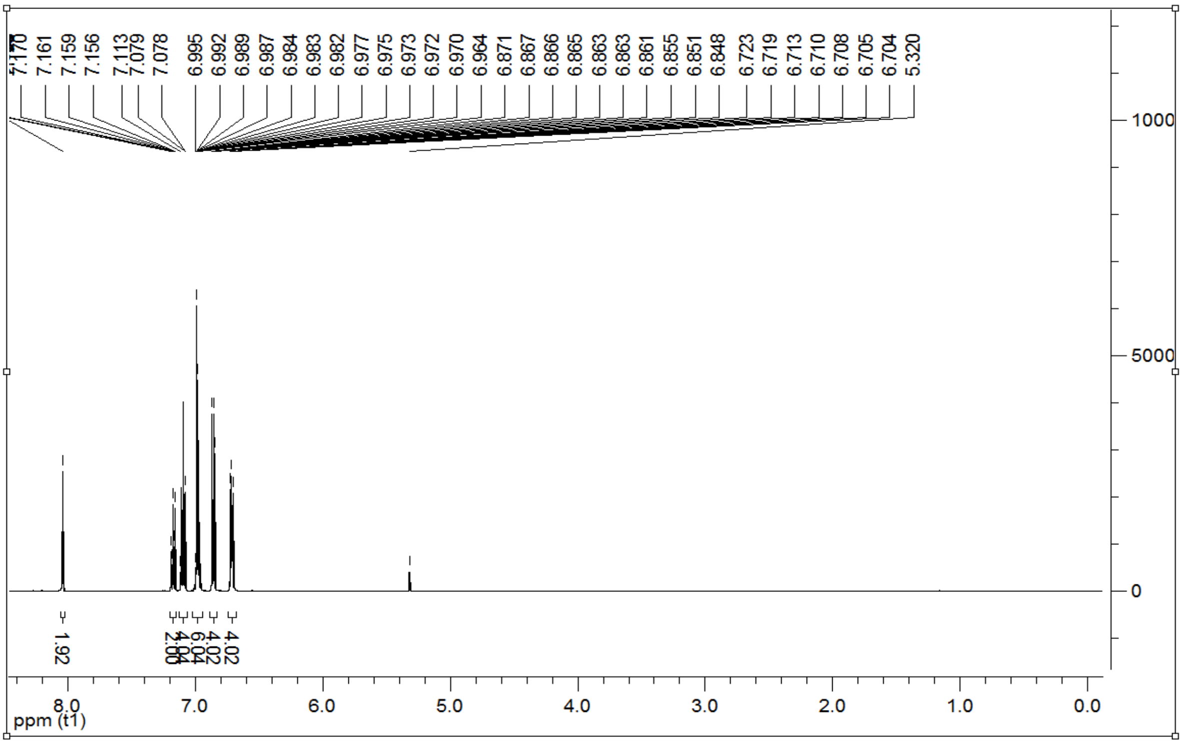

Fig. S15 ^{1}H NMR spectrum of **1** in CD_2Cl_2 at 500 MHz.

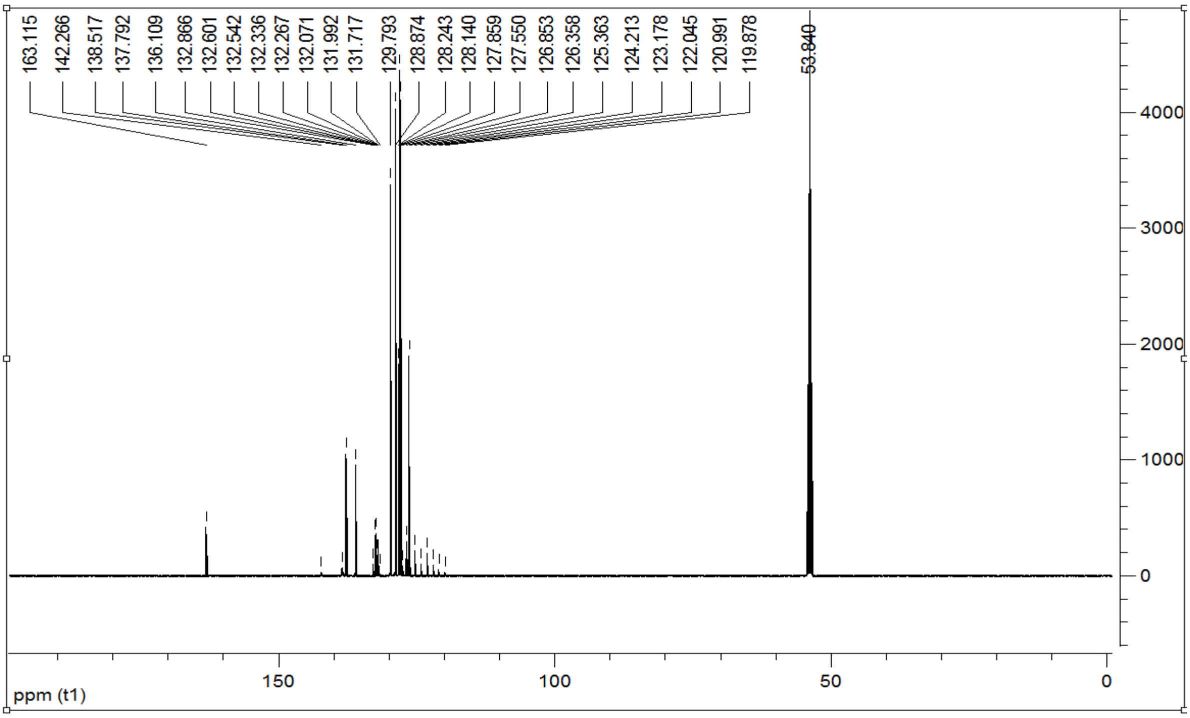

Fig. S16 $^{13}C\{^{1}H\}$ NMR spectrum of **1** in CD_2Cl_2 at 125 MHz.

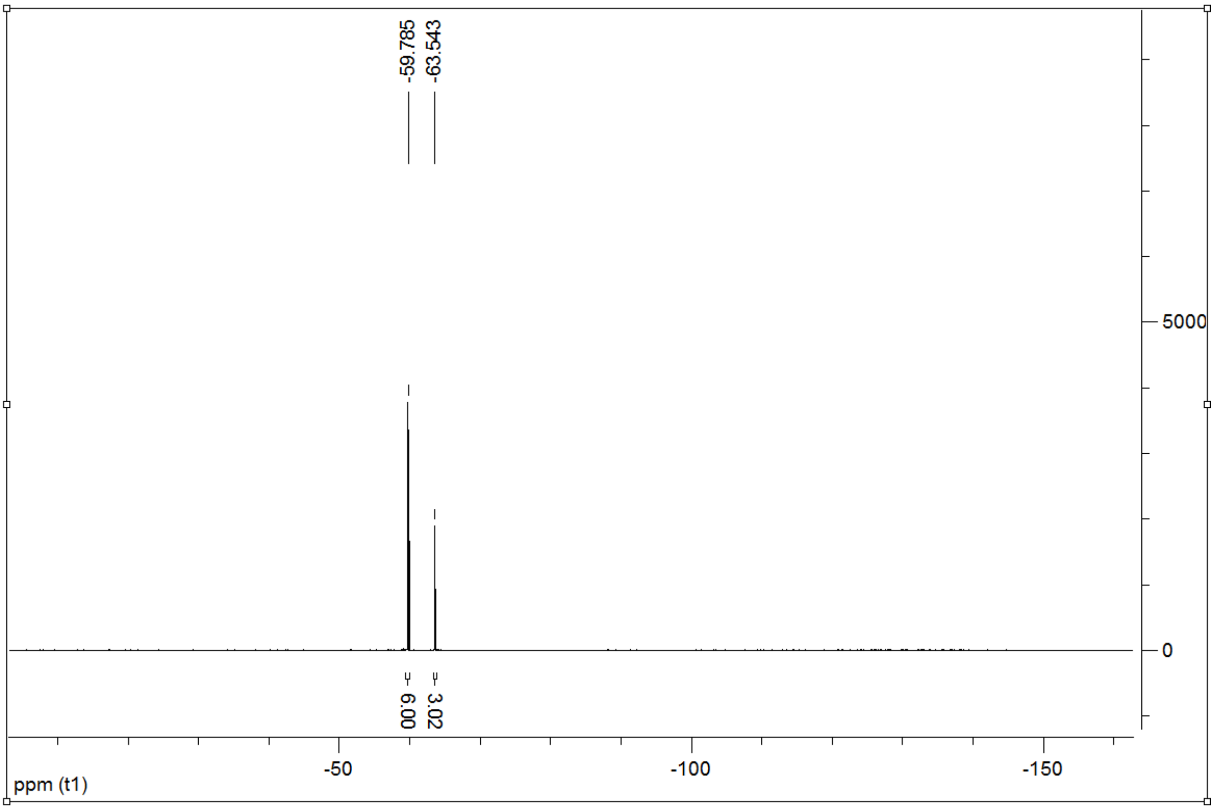

Fig. S17 $^{19}F\{^1H\}$ NMR spectrum of **1** in CD_2Cl_2 at 188 MHz.

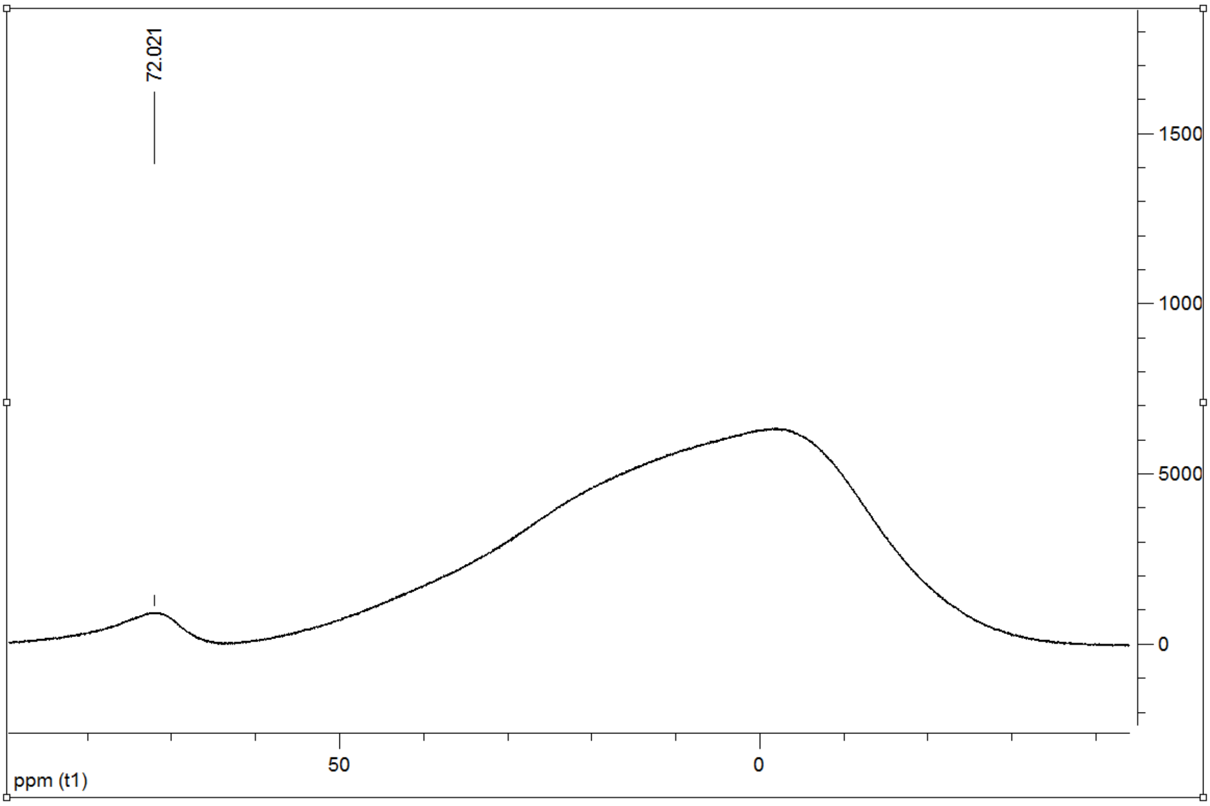

Fig. S18 ^{11}B NMR spectrum of **1** in CD_2Cl_2 at 160 MHz.

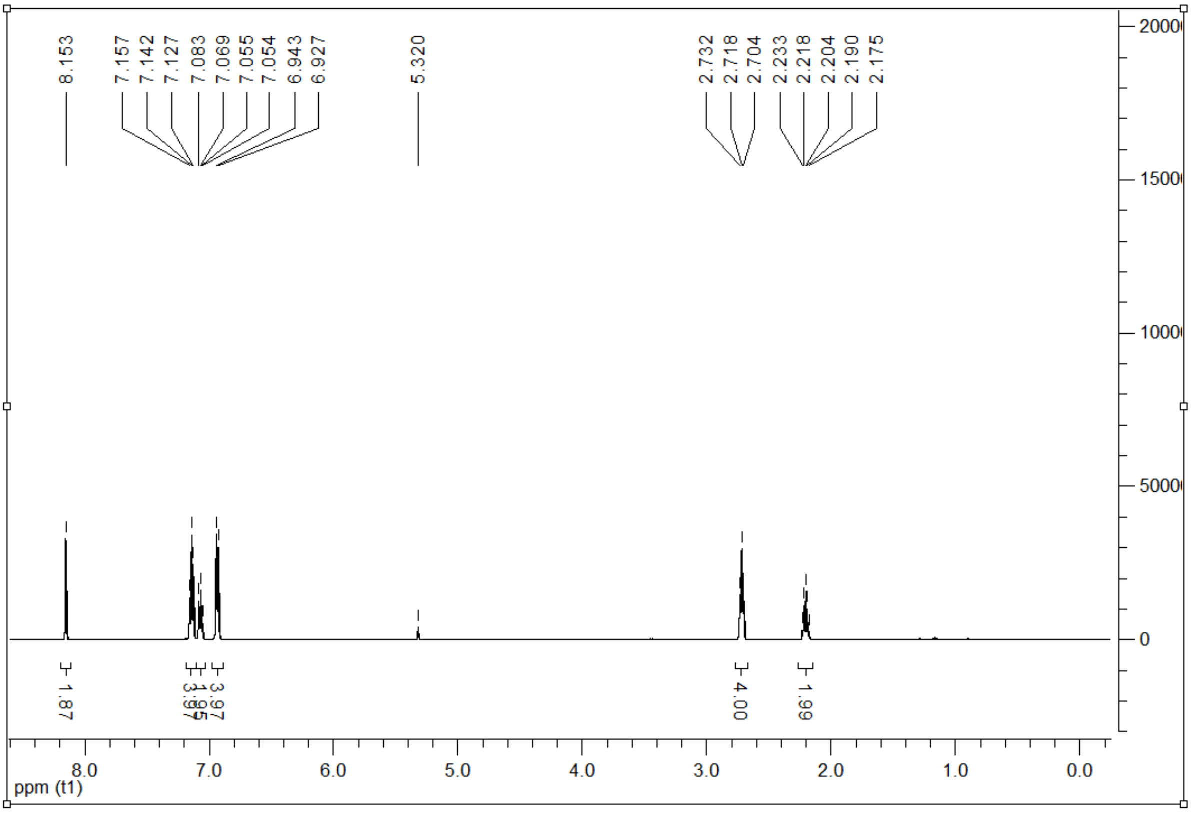

Fig. S19 ^{1}H NMR spectrum of **2** in CD_2Cl_2 at 500 MHz.

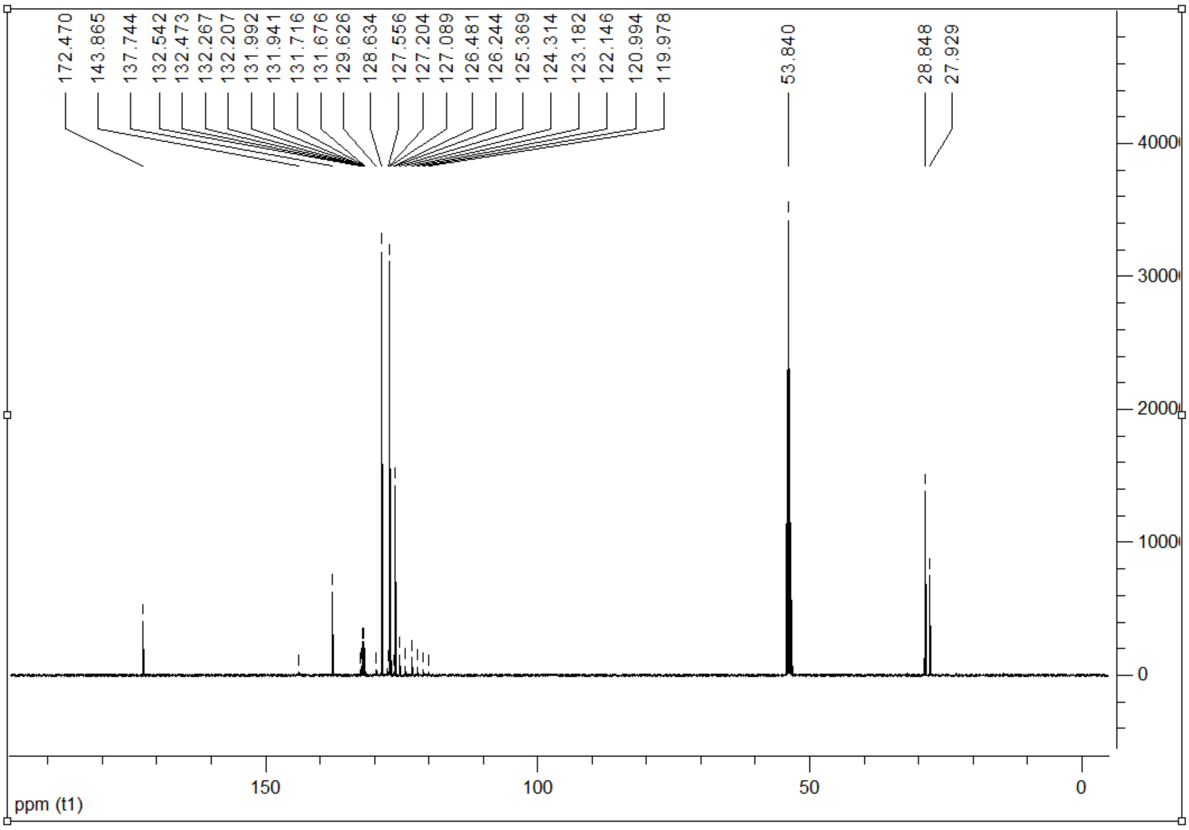

Fig. S20 $^{13}C\{^1H\}$ NMR spectrum of **2** in CD_2Cl_2 at 125 MHz.

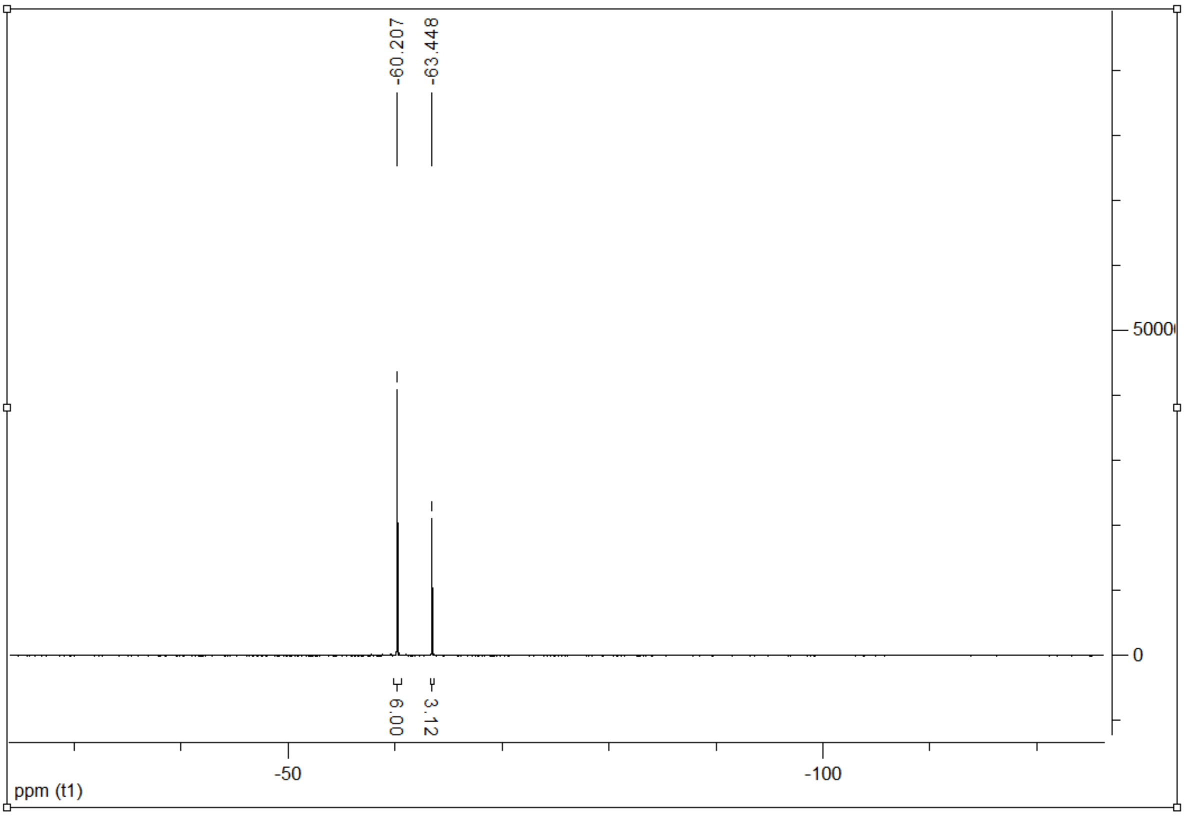

Fig. S21 $^{19}F\{^1H\}$ NMR spectrum of **2** in CD_2Cl_2 at 188 MHz.

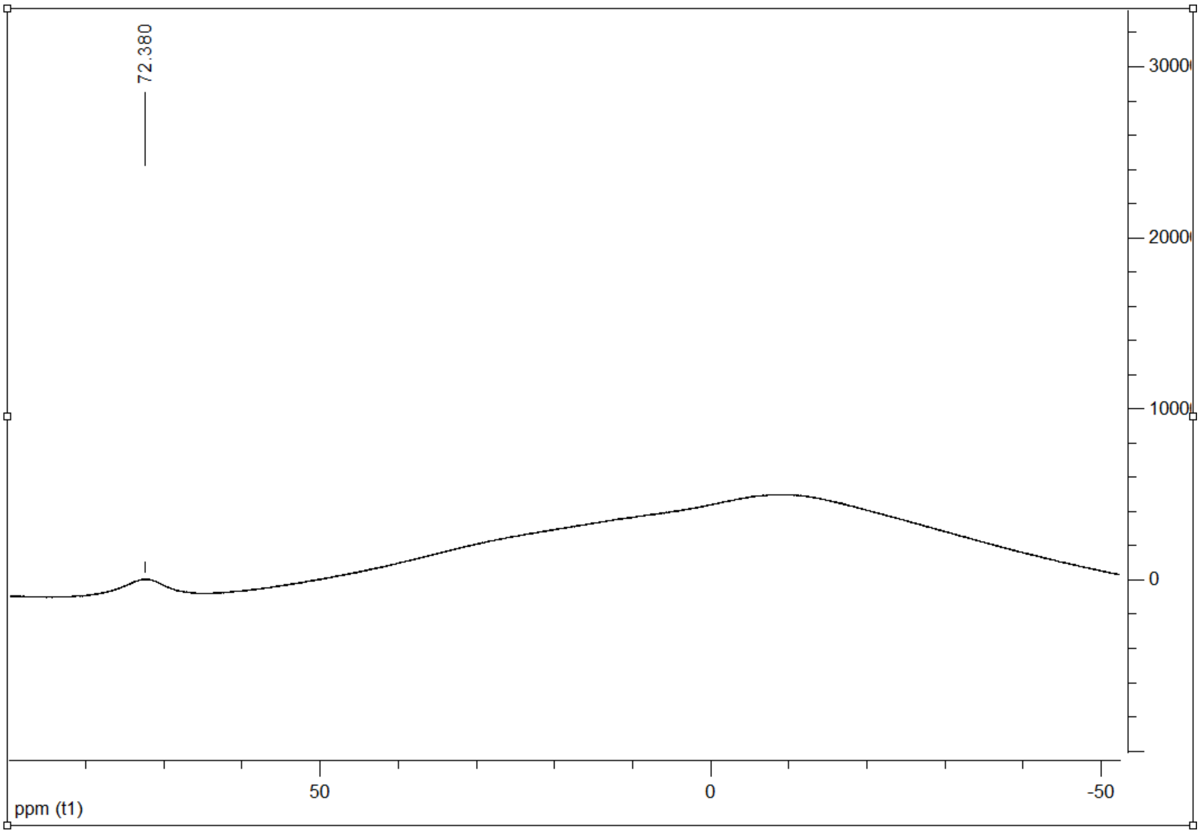

Fig. S22 ^{11}B NMR spectrum of **2** in CD_2Cl_2 at 160 MHz.

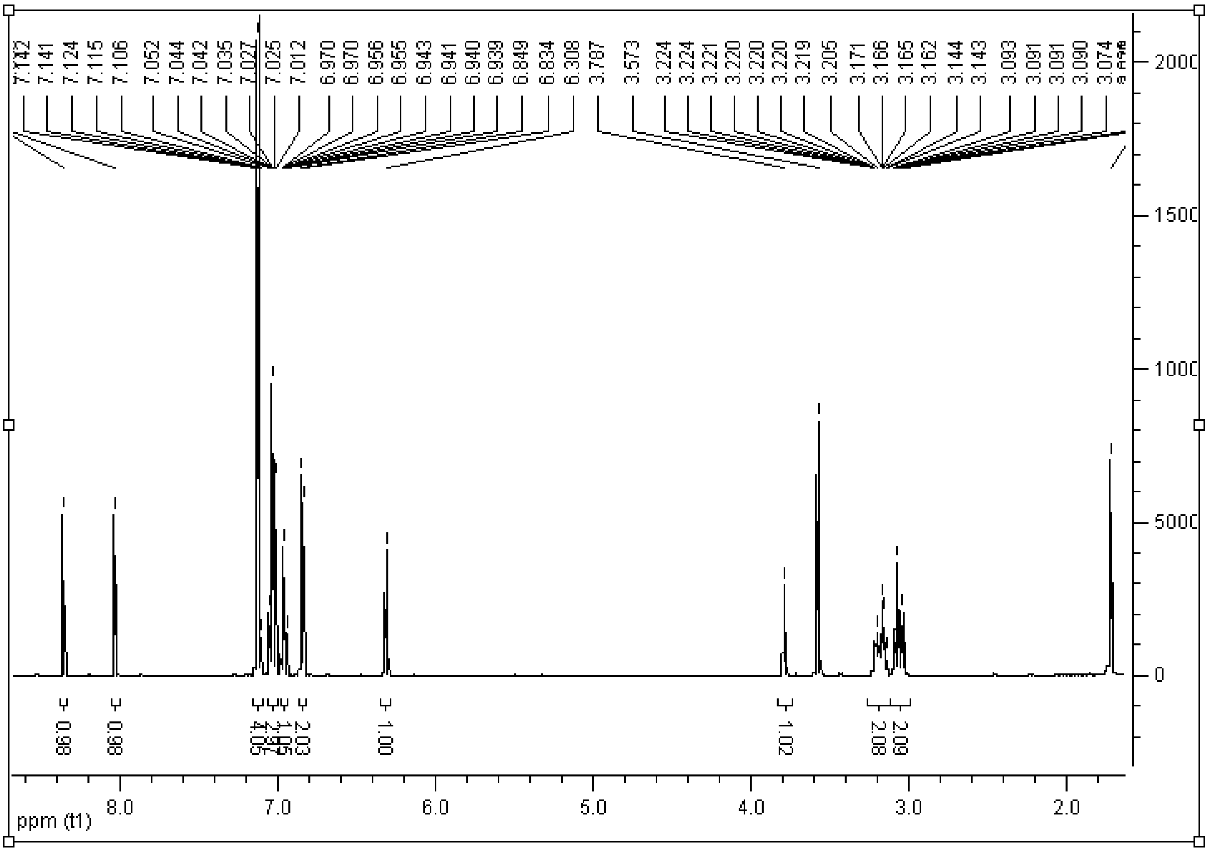

Fig. S23 ^{1}H NMR spectrum of **5** in THF-d_8 at 500 MHz.

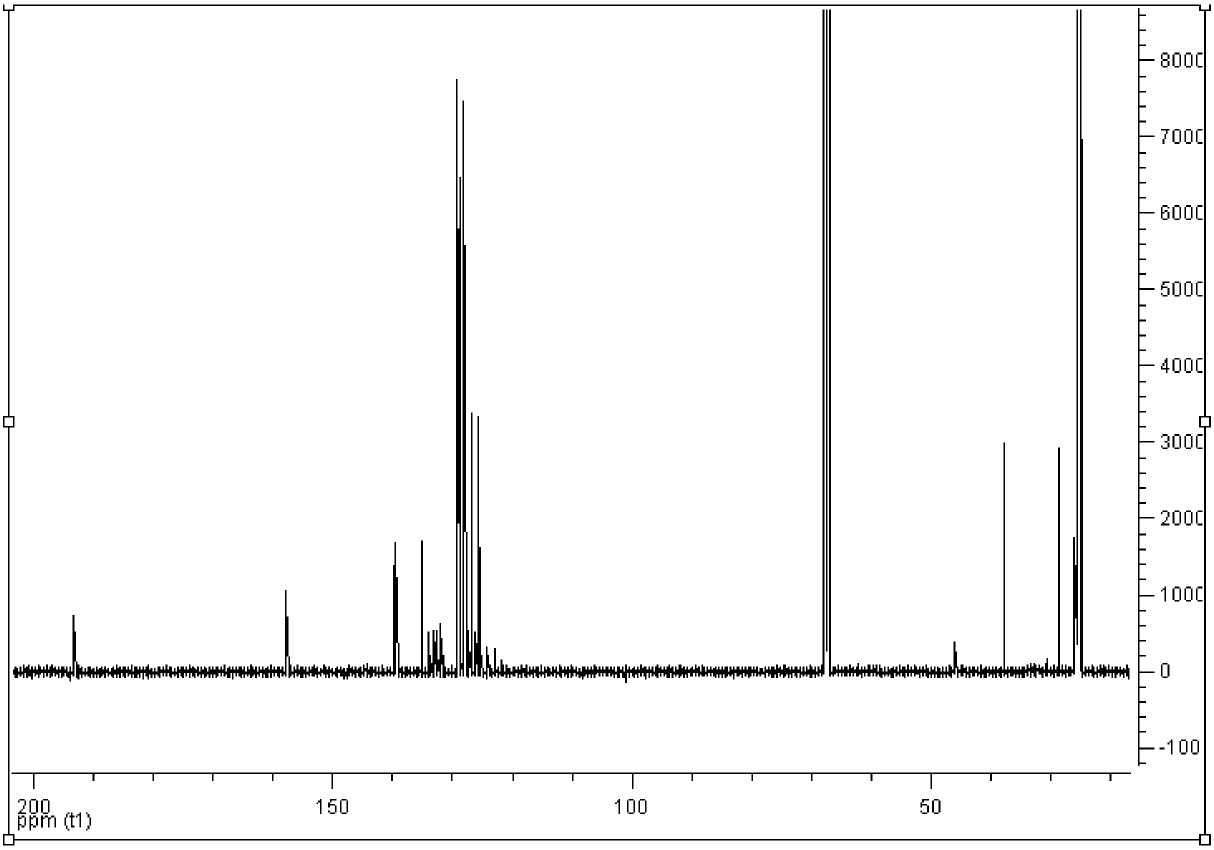

Fig. S24 ^{13}C{^{1}H} NMR spectrum of **5** in THF-d_8 at 125 MHz.

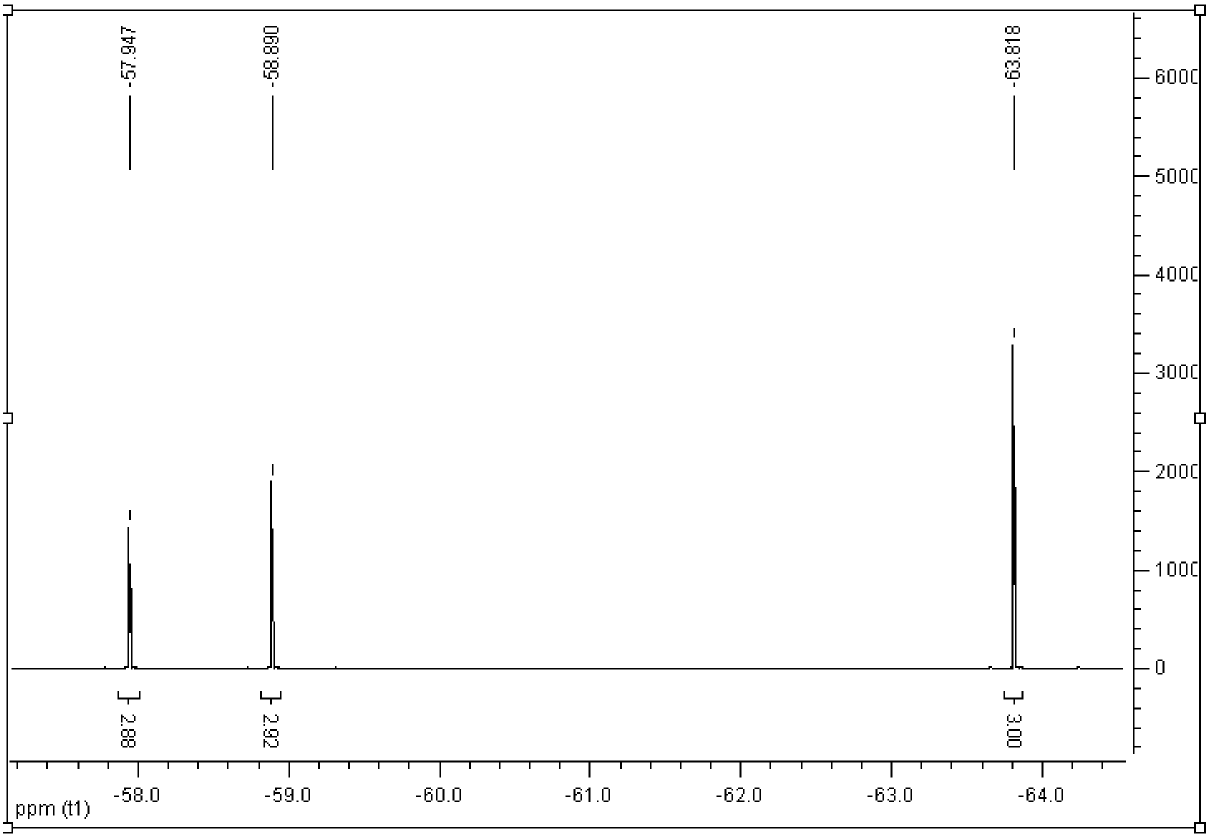

Fig. S25 ^{19}F NMR spectrum of **5** in THF-d_8 at 470 MHz.

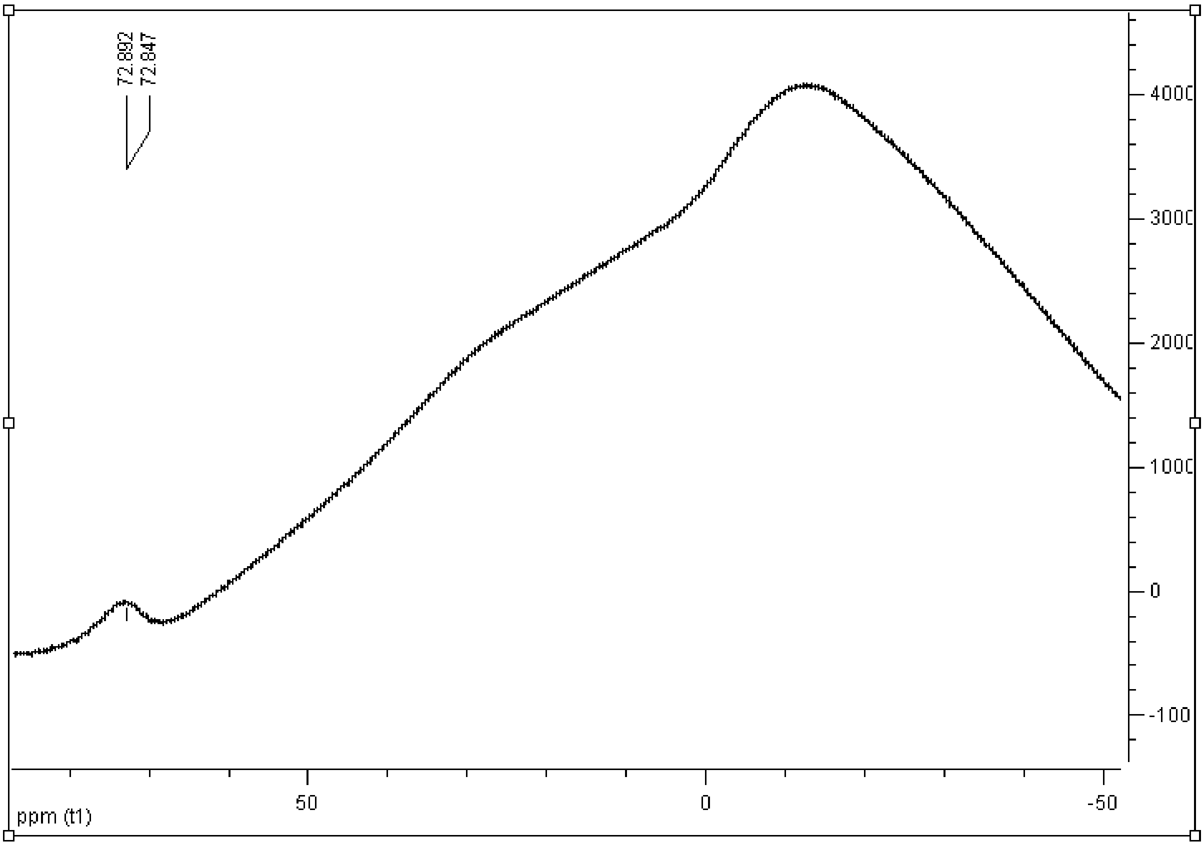

Fig. S26 ^{11}B NMR spectrum of **5** in THF-d_8 at 160 MHz.

NMR and GC-MS analyses of the hydrolysis process of $MesBC_4Ph_4$, 1 and 2 in wet CD_2Cl_2 and in air; single-crystal X-ray diffraction of hydrolysed 2

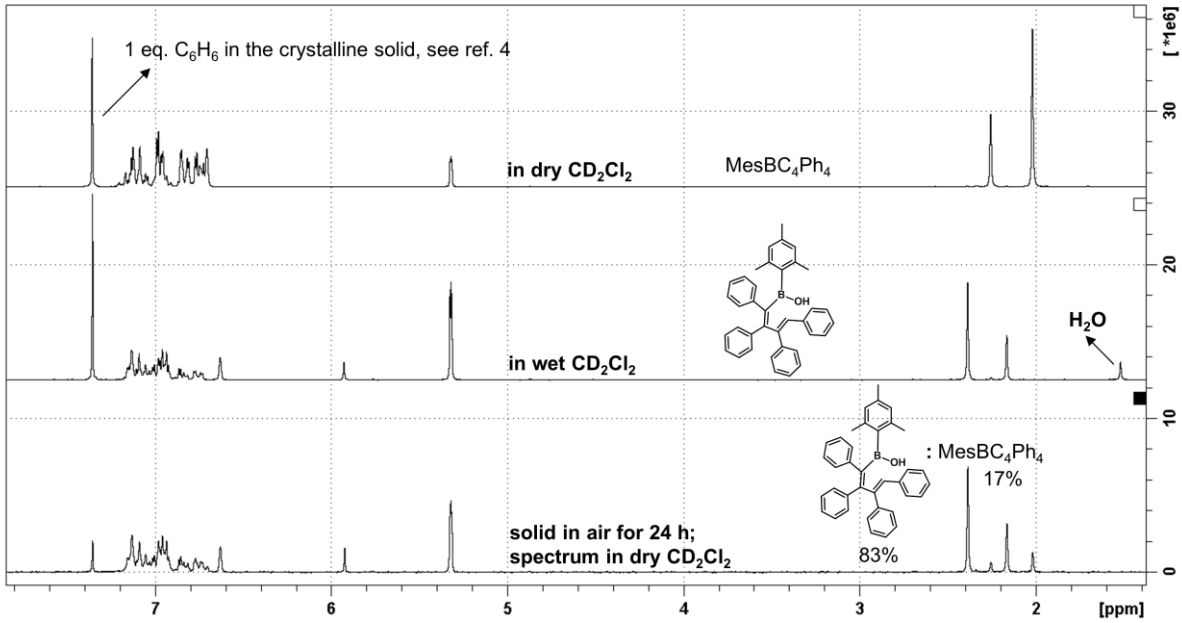

Fig. S27 ^{1}H NMR spectra (200 MHz) showing the hydrolysis of $MesBC_4Ph_4$ in wet CD_2Cl_2 and after exposure of a solid sample to air for 24 h.

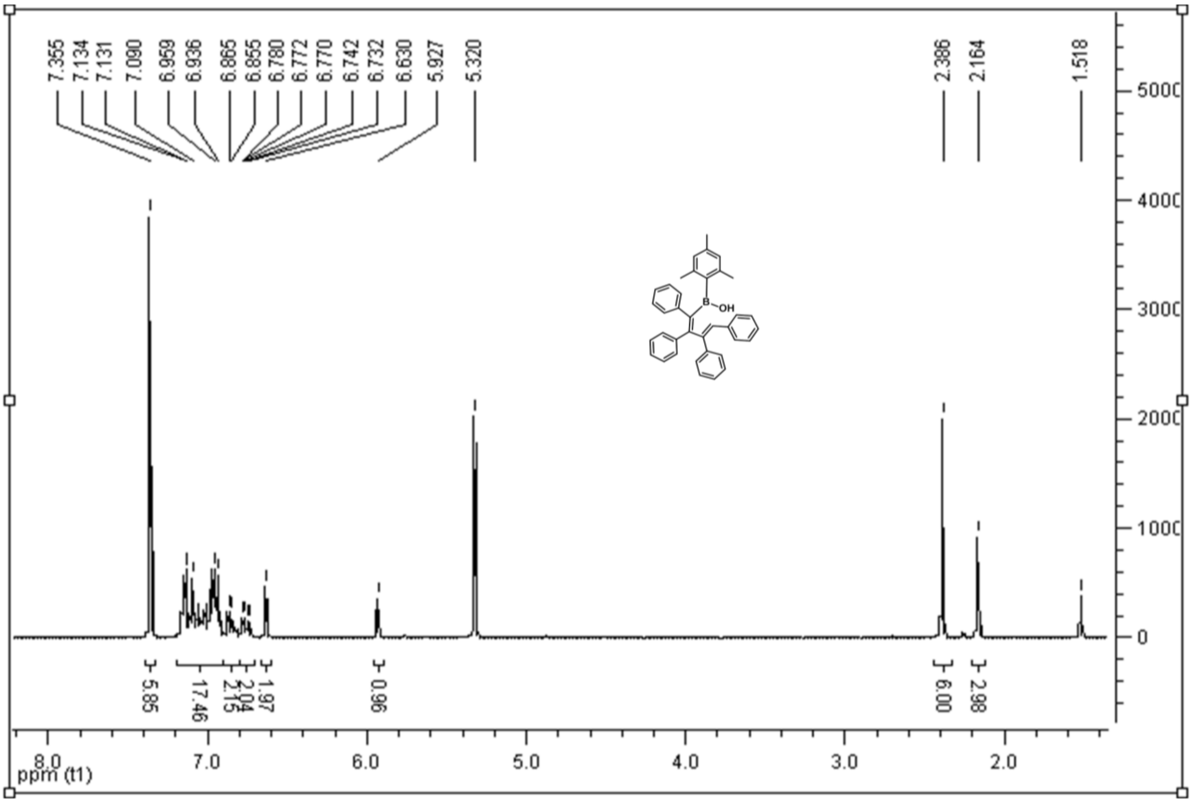

Fig. S28 ^{1}H NMR spectrum (200 MHz) of $MesBC_4Ph_4$ in wet CD_2Cl_2. $MesBC_4Ph_4$ was totally hydrolysed.

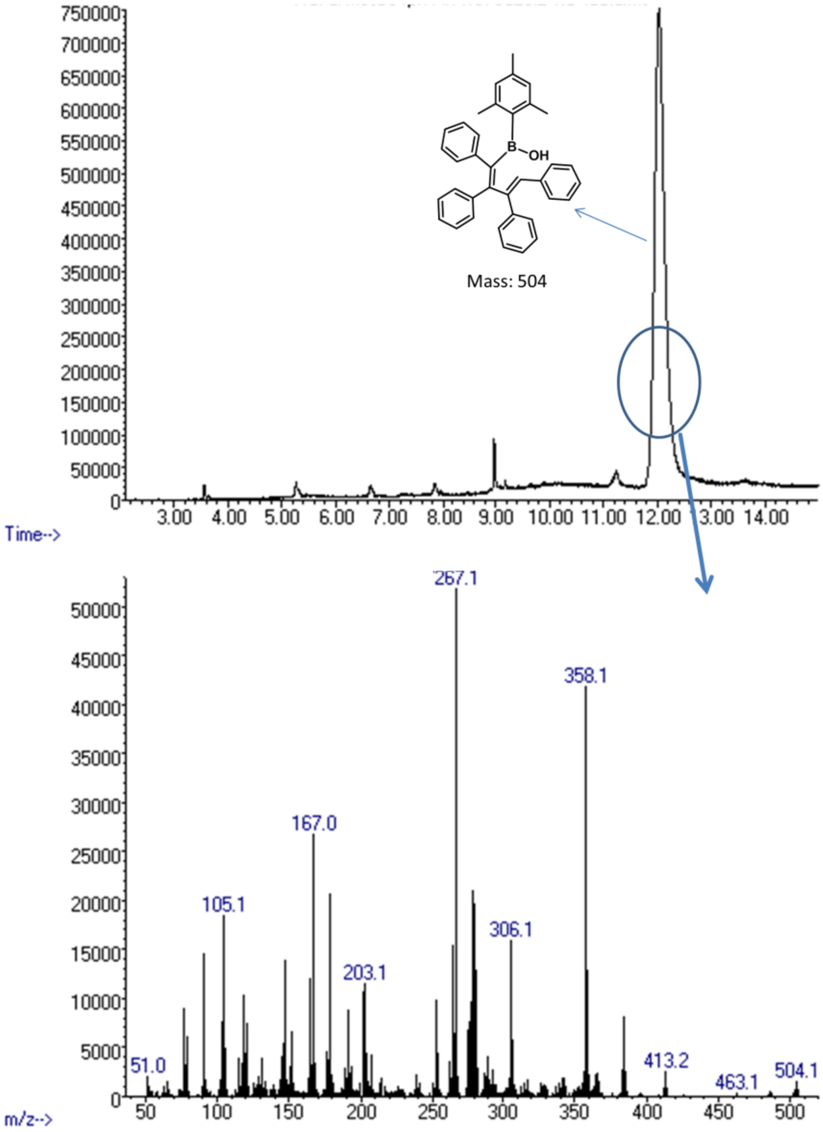

Fig. S29 GC trace (top) and an EI$^+$ mass spectrum (bottom) of a solution of $MesBC_4Ph_4$ in wet CD_2Cl_2. $MesBC_4Ph_4$ was totally hydrolysed.

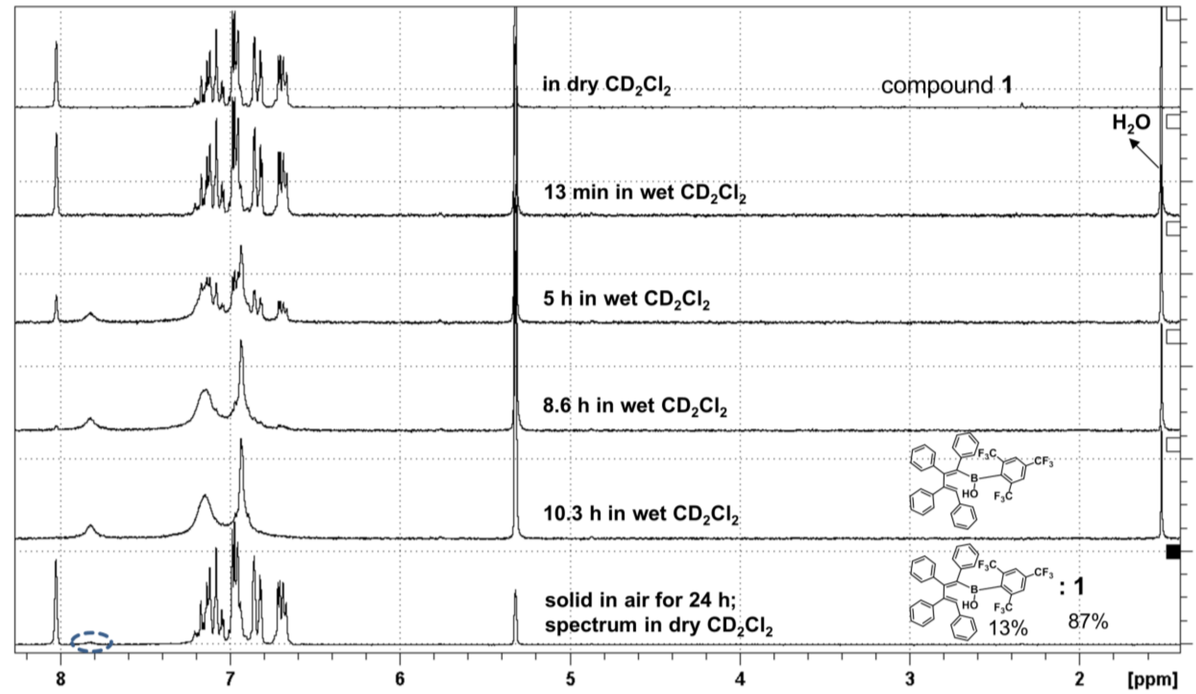

Fig. S30 ^{1}H NMR spectra (200 MHz) showing the hydrolysis of **1** in wet CD_2Cl_2 and after exposure of a solid sample to air for 24 h.

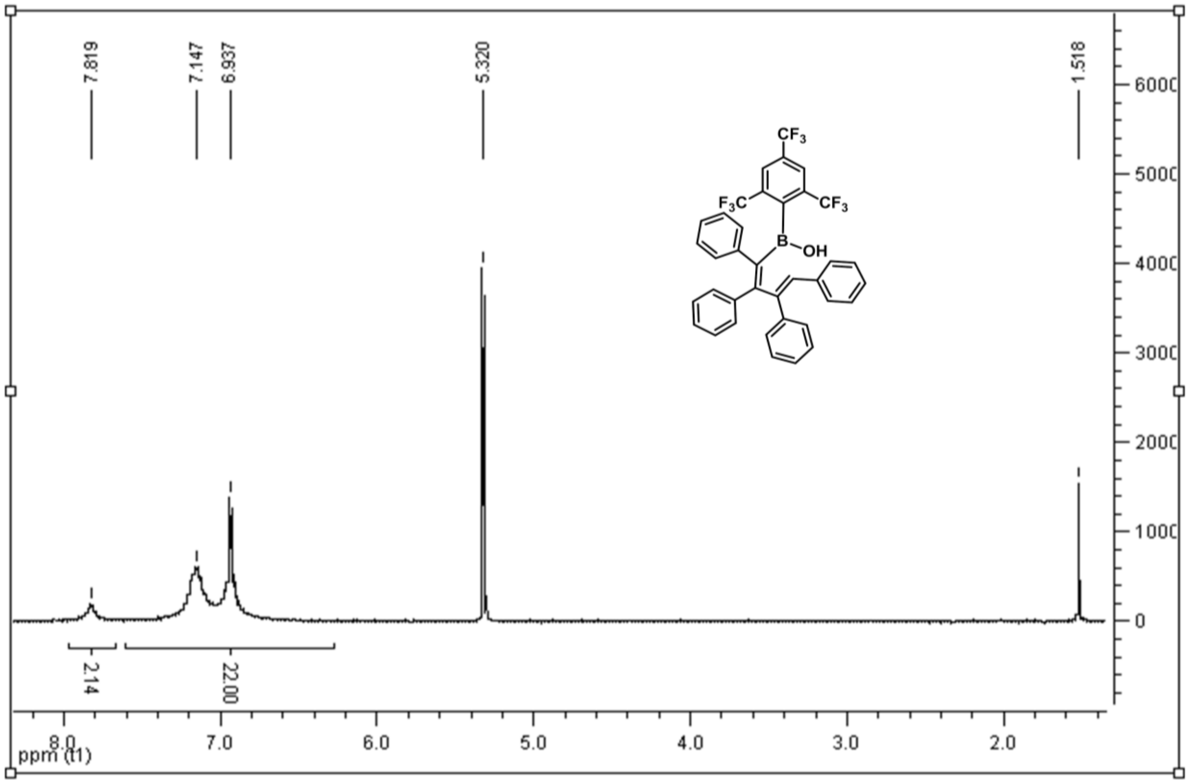

Fig. S31 ^{1}H NMR spectrum (200 MHz) of **1** measured after the compound was stored in wet CD_2Cl_2 for 10.3 h. **1** was totally hydrolysed.

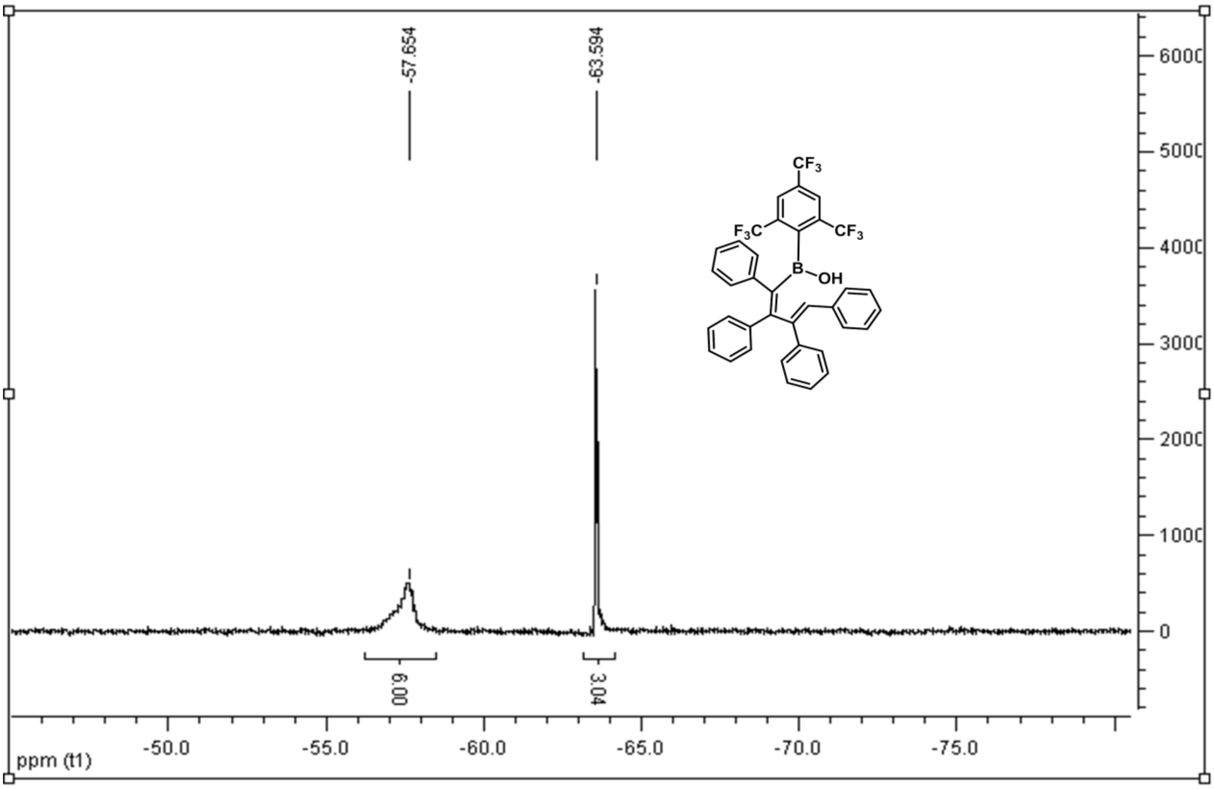

Fig. S32 $^{19}F\{^1H\}$ NMR spectrum (188 MHz) of **1** measured after the compound was stored in wet CD_2Cl_2 for 10.3 h. **1** was totally hydrolysed

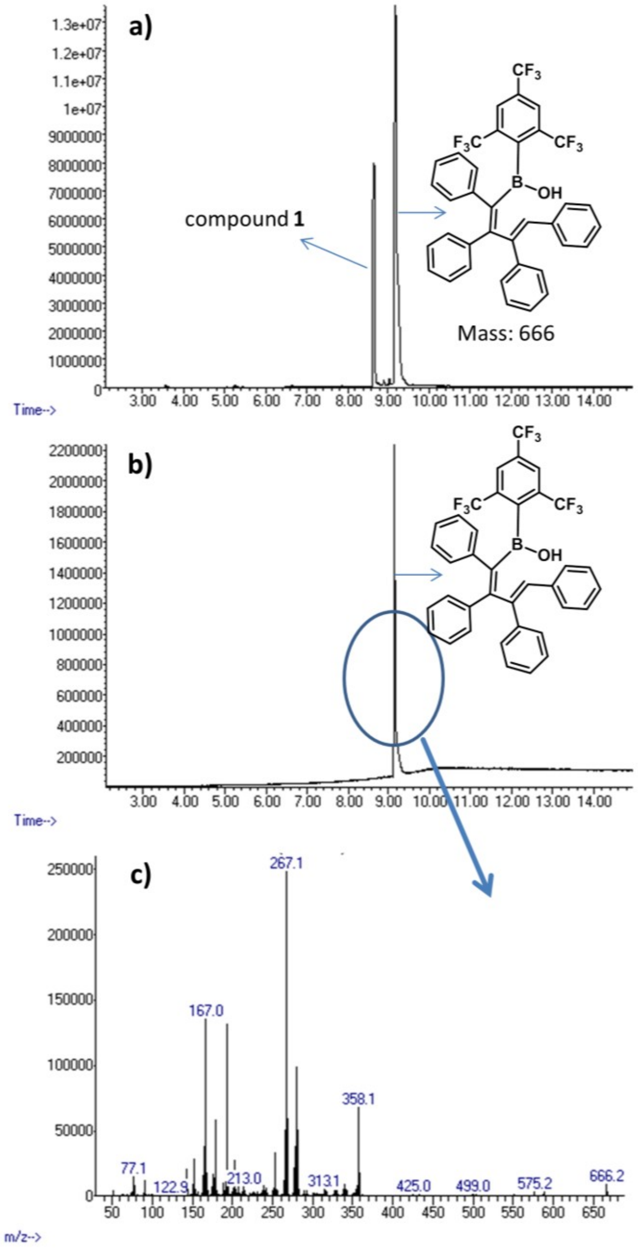

Fig. S33 a) GC trace of a solution of **1** in wet CD_2Cl_2 showing the partial hydrolysis of **1**; b) GC trace of the totally hydrolysed solid sample of **1** obtained after storing a crystalline sample **1** under air for *ca.* 2–3 weeks; c) Mass spectrum of the hydrolysed product of **1**.

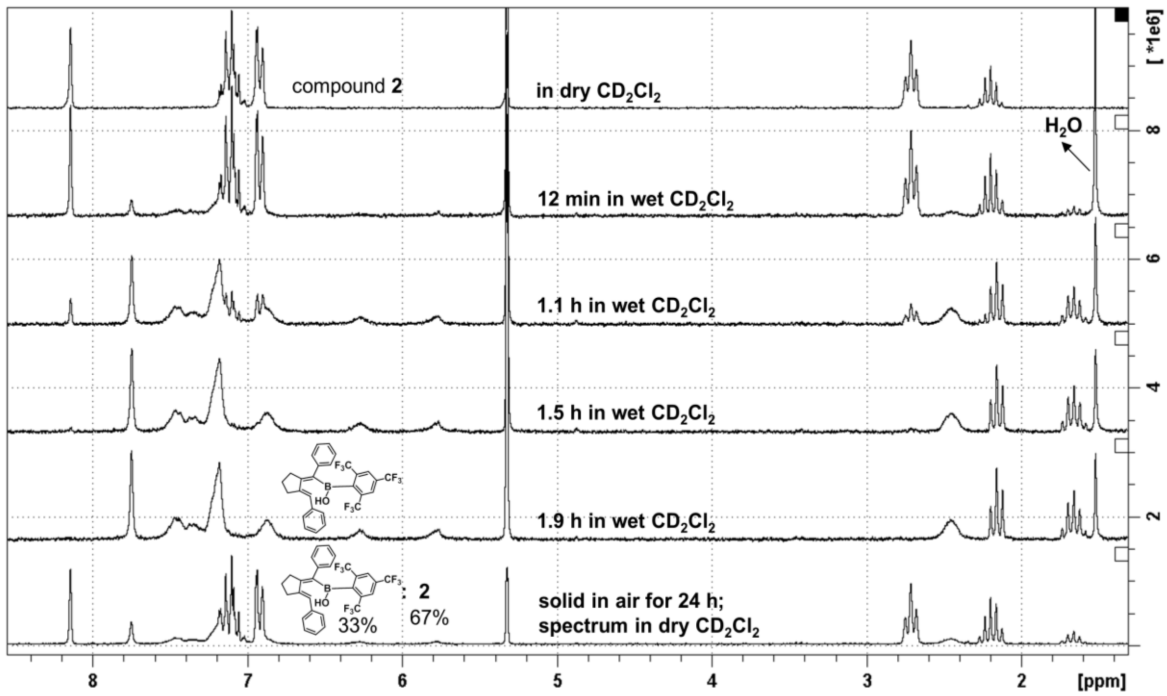

Fig. S34 ^{1}H NMR spectra (200 MHz) showing the hydrolysis of **2** in wet CD_2Cl_2 and after exposure of a solid sample to air for 24 h.

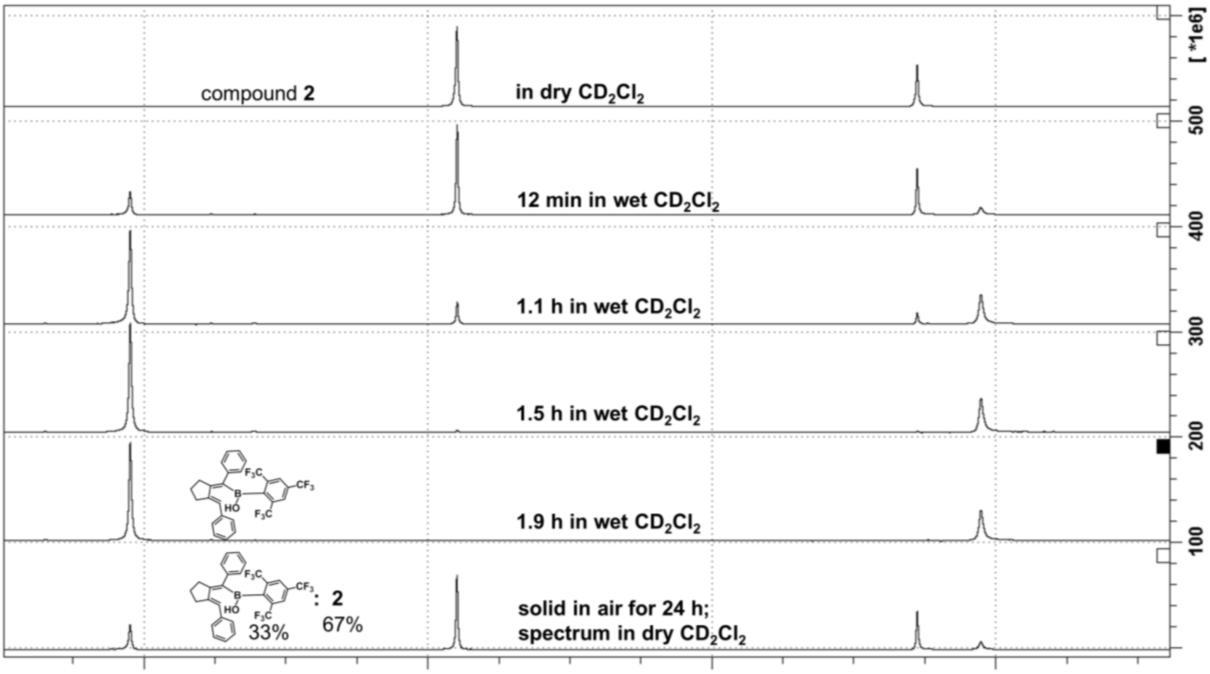

Fig. S35 ^{19}F{^{1}H} NMR spectra (188 MHz) showing the hydrolysis of **2** in wet CD_2Cl_2 and after exposure of a solid sample to air for 24 h.

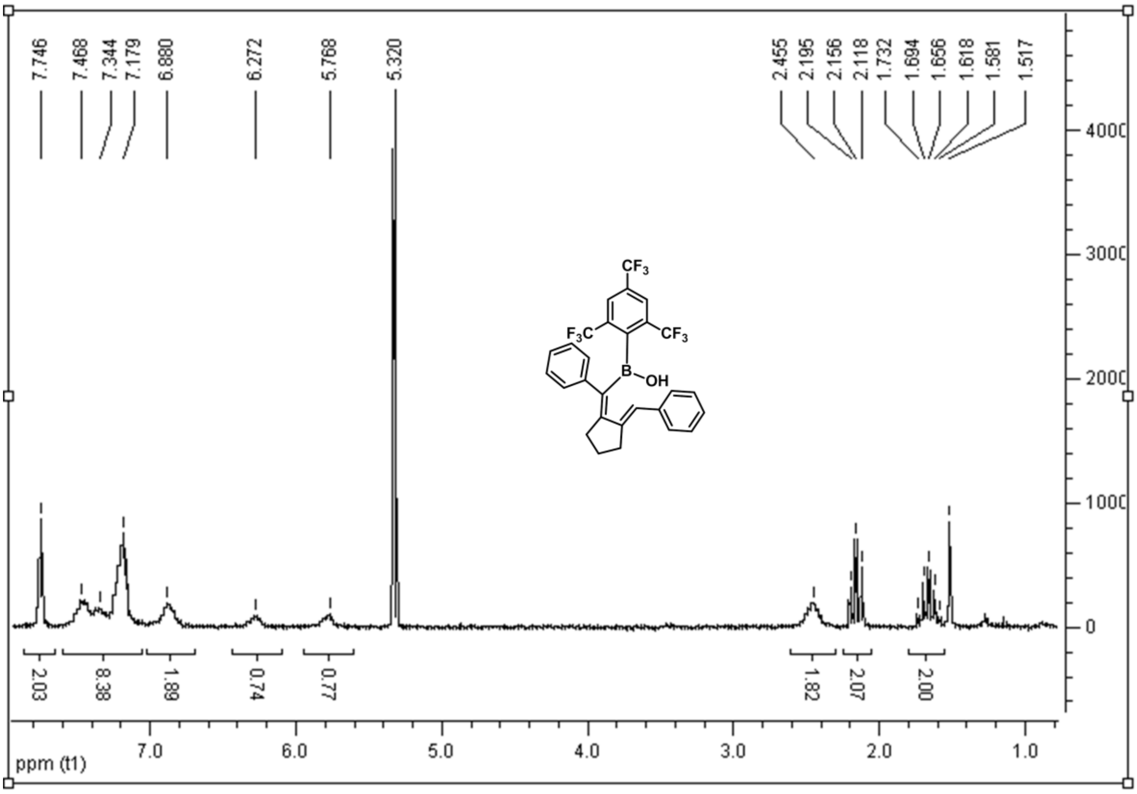

Fig. S36 ^{1}H NMR spectrum (200 MHz) of **2** measured after the compound was stored in wet CD_2Cl_2 for 1.9 h. **2** was totally hydrolysed.

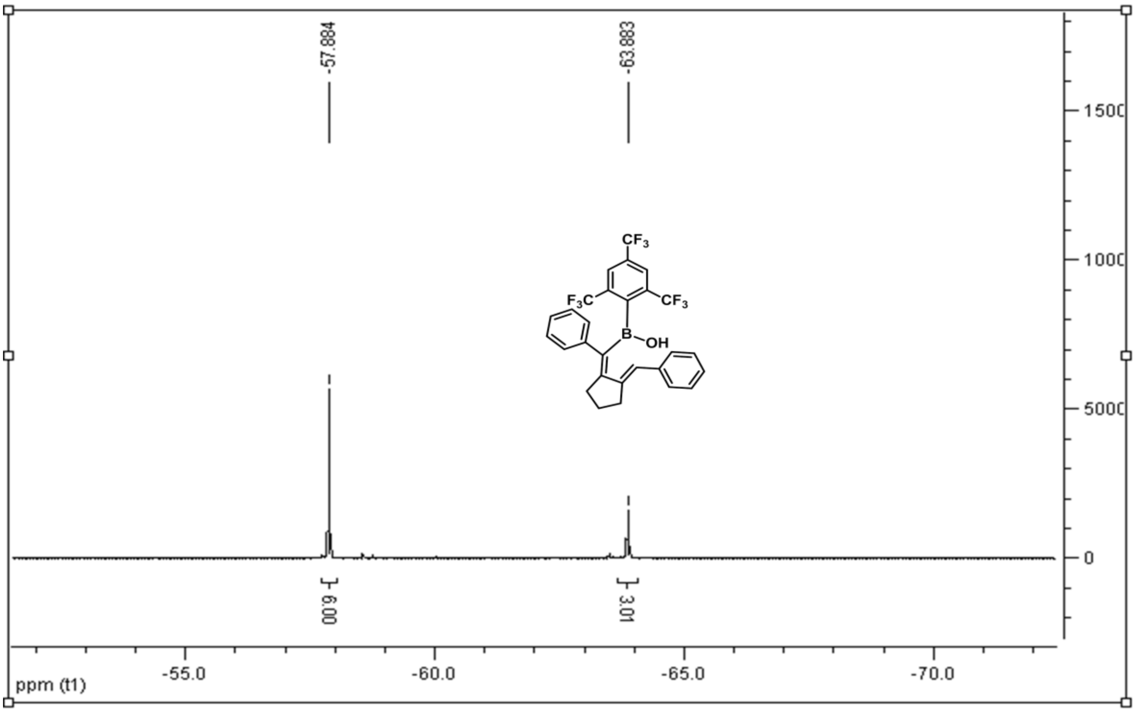

Fig. S37 $^{19}F\{^1H\}$ NMR spectrum (188 MHz) of **2** measured after the compound was stored in wet CD_2Cl_2 for 1.9 h. **2** was totally hydrolysed.

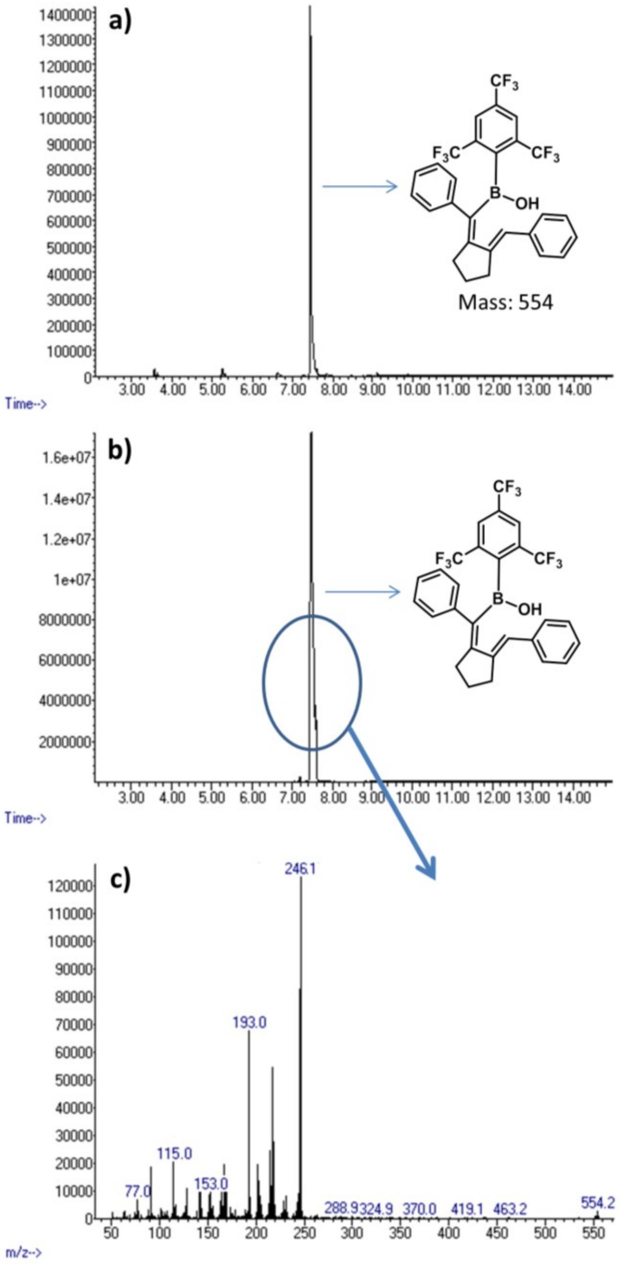

Fig. S38 a) GC trace of a solution of **2** in wet CD_2Cl_2 measured after its total hydrolysis**;** b) GC trace of the totally hydrolysed solid sample of **2** obtained after storing a crystalline sample of **2** under air for *ca.* 2–3 weeks: c) Mass spectrum of the hydrolysed product of **2**.

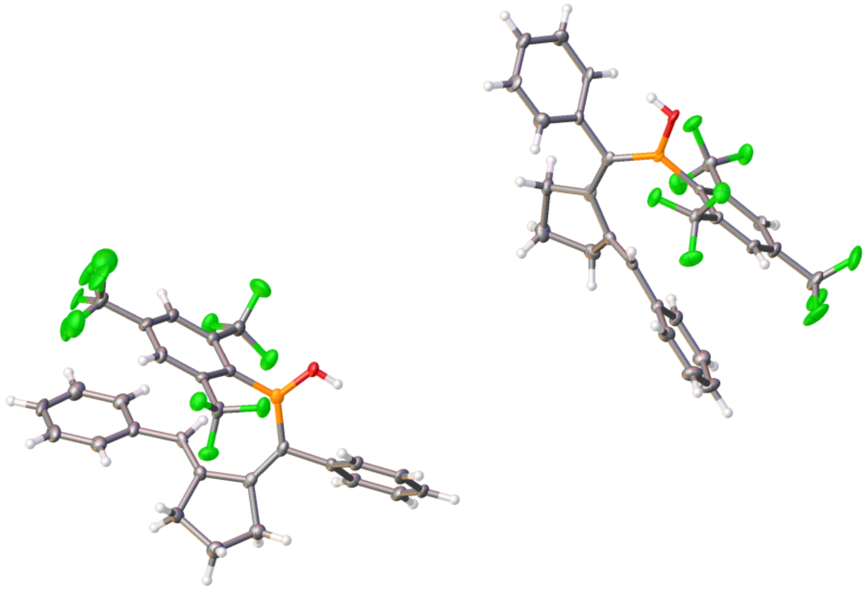

Fig. S39 The molecular structure of hydrolysed **2** as determined by X-ray crystallography. Atom colour code: carbon (grey), fluorine (green), boron (orange), oxygen (red), hydrogen (white). Atomic displacement ellipsoids are drawn at 50% probability.

Crystal Data: $C_{28}H_{20}BF_9O$, $M_r = 554.25$, Bruker APEX-II CCD none, monoclinic, $P2_1/n$, $a = 8.6666(11)$ Å, $b = 35.693(5)$ Å, $c = 15.690(2)$ Å, $\beta = 91.689(4)°$, $V = 4851.2(11)$ Å^3, $Z = 8$, $\rho_{calcd} = 1.518$ g cm^{-3}, $\mu = 0.138$ mm^{-1}, $F(000) = 2256$, $T = 100(2)$ K, $R_1 = 0.1040$, $wR_2 = 0.1773$, 8682 independent reflections [$2\theta \leq 50.1°$] and 734 parameters.

Thermal analyses of 1 and 2

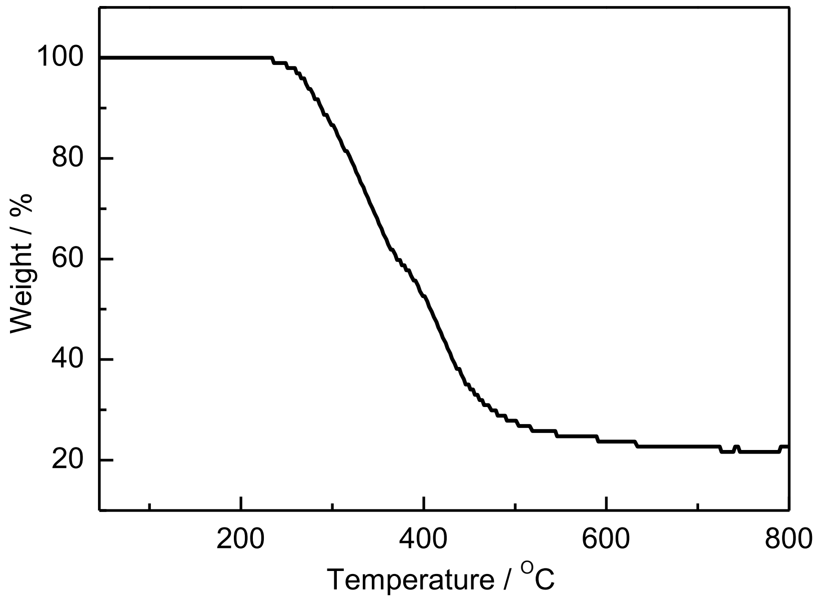

Fig. S40 TGA trace of **1** measured at a heating rate of 10 °C min^{-1}.

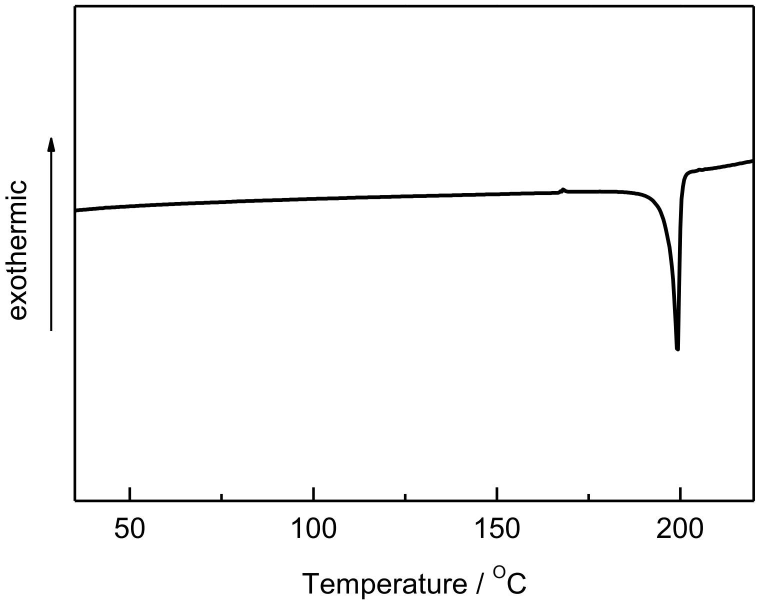

Fig. S41 DSC trace of **1** measured at a heating rate of 10 °C min^{-1}.

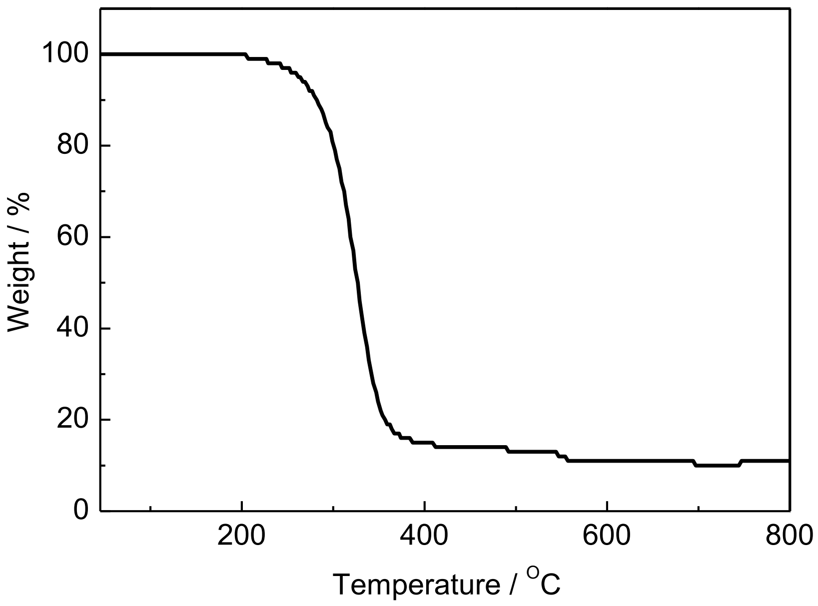

Fig. 42 TGA trace of **2** measured at a heating rate of 10 °C min^{-1}.

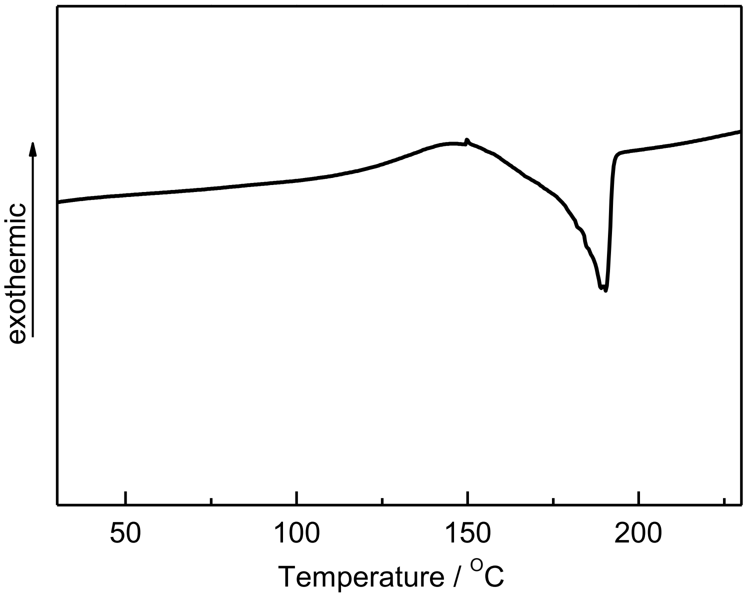

Fig. S43 DSC trace of **2** measured at a heating rate of 10 °C min^{-1}.

GC-MS of 1 and 2

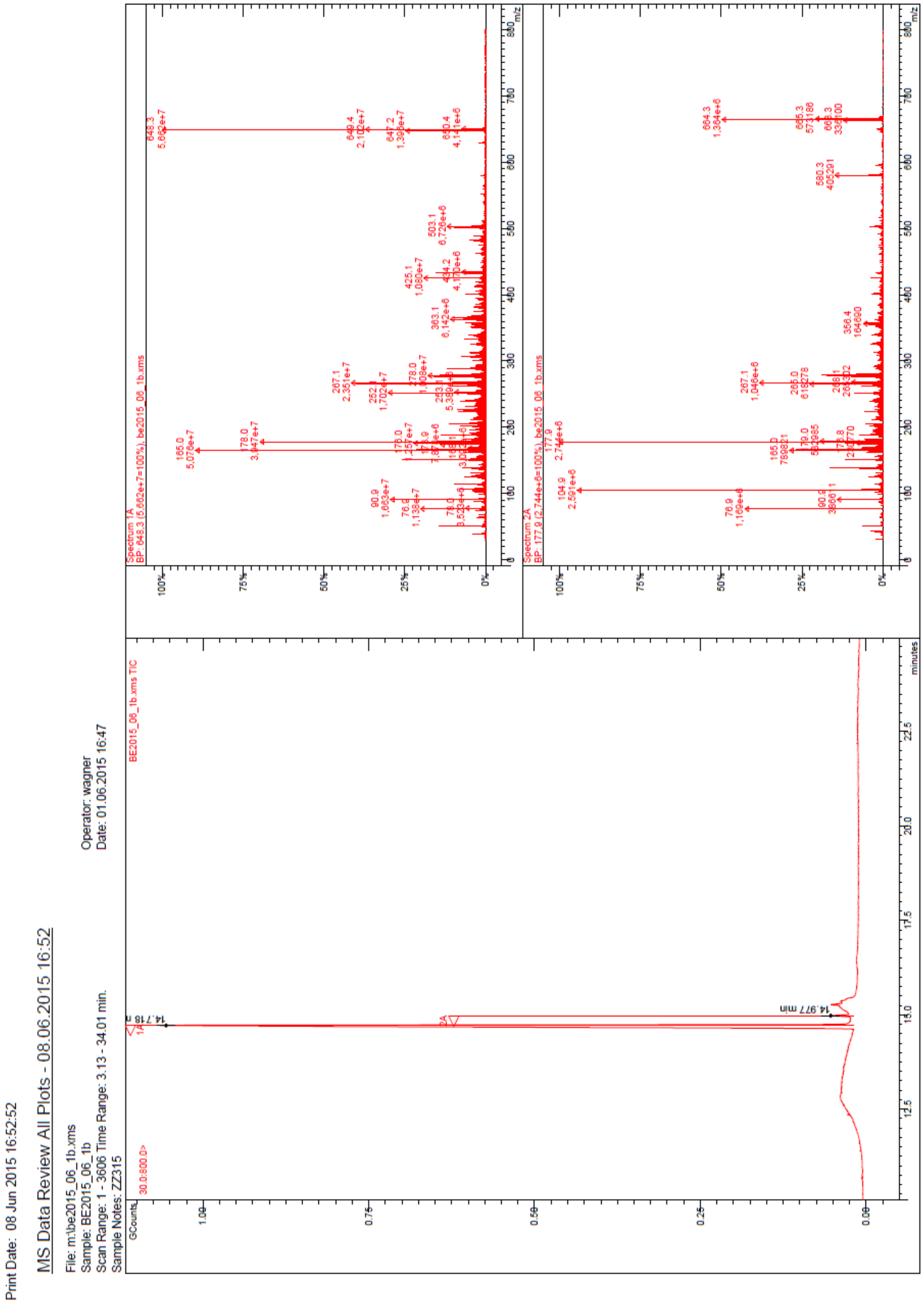

Fig. S44 GC trace and mass spectrum of **1**

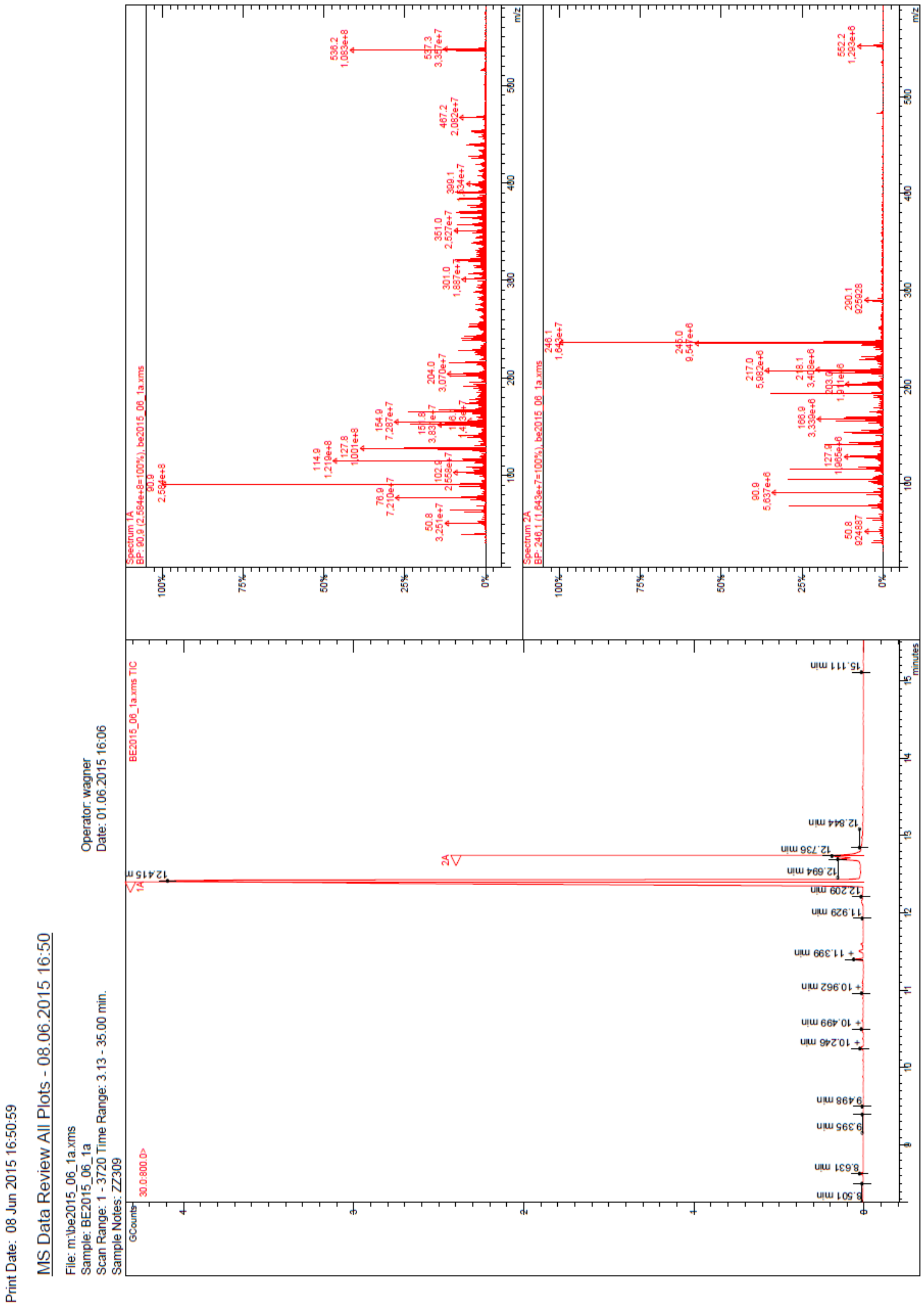
Print Date: 08 Jun 2015 16:50:59

MS Data Review All Plots - 08.06.2015 16:50

File: m:\be2015_06_1a.xms
Sample: BE2015_06_1a
Scan Range: 1 - 3720 Time Range: 3.13 - 35.00 min.
Sample Notes: ZZ309

Operator: wagner
Date: 01.06.2015 16:06

Fig. S45 GC trace and mass spectrum of **2**

NMR spectra showing the reversible binding of 1 and 2 with pyridine

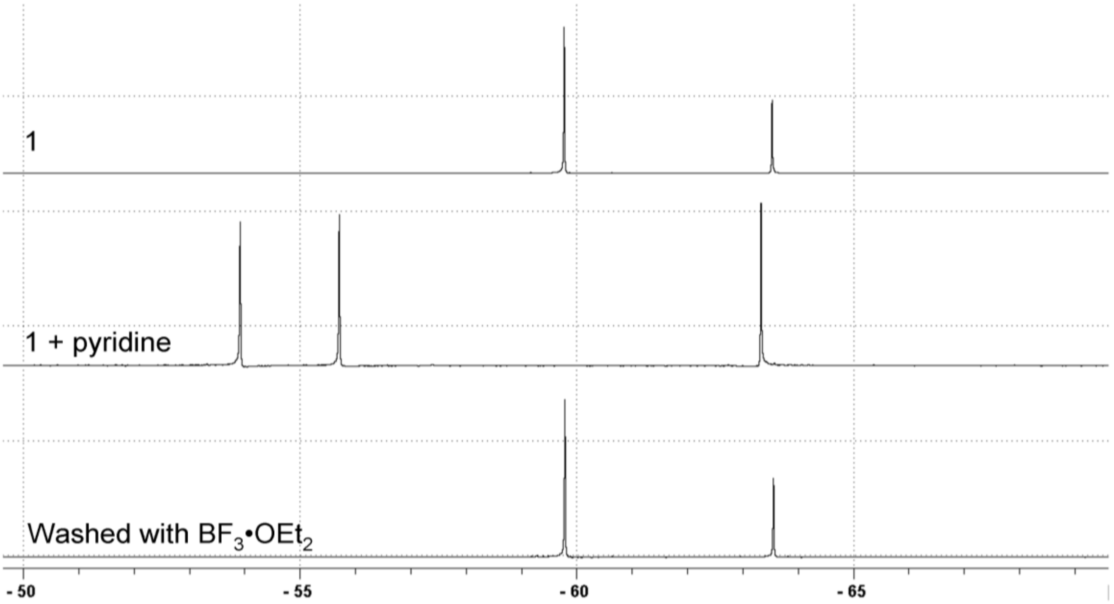

Fig. S46 $^{19}F\{^1H\}$ NMR spectra (188 MHz) showing the reversible binding of pyridine with compound **1** in CD_2Cl_2.

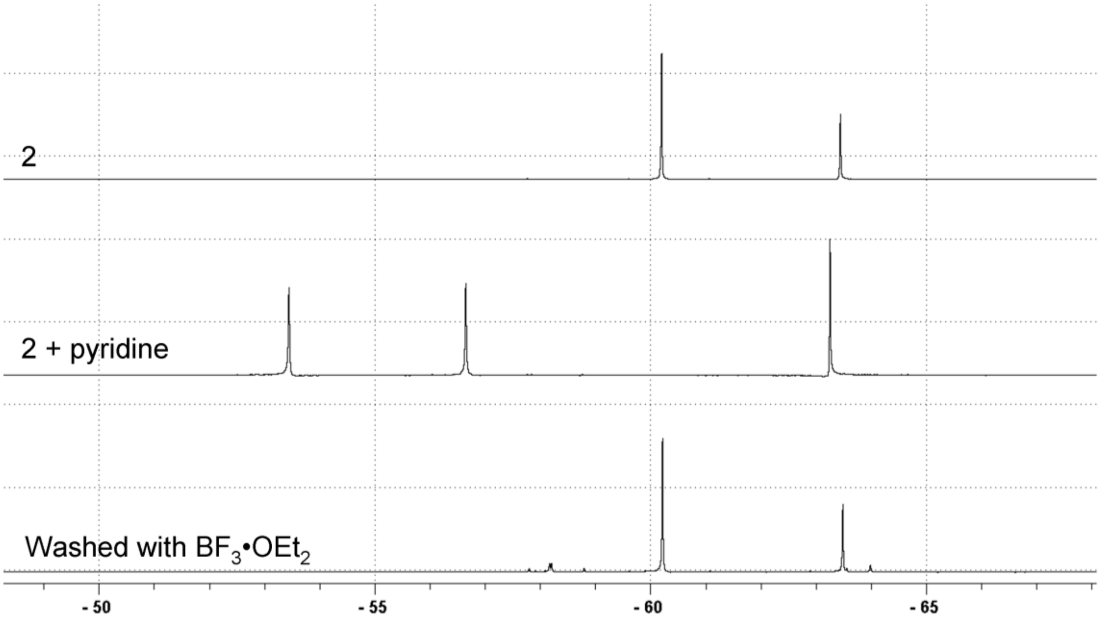

Fig. S47 $^{19}F\{^1H\}$ NMR spectra (188 MHz) showing the reversible binding of pyridine with compound **2** in CD_2Cl_2.

References

[1] G. E. Carr, R. D. Chambers, T. F. Holmes, *J. Organomet. Chem.* 1987, **325**, 13–23.

[2] E. Negishi, S. J. Holmes, J. M. Tour, J. A. Miller, F. E. Cederbaum, D. R. Swanson, T. Takahashi, *J. Am. Chem. Soc.* 1989, **111**, 3336–3346.

[3] S. Yamaguchi, R.-Z. Jin, K. Tamao, F. Sato, *J. Org. Chem.* 1998, **63**, 10060–10062.

[4] H. Braunschweig, V. Dyakonov, J. O. C. Jimenez-Halla, K. Kraft, I. Krummenacher, K. Radacki, A. Sperlich, J. Wahler, *Angew. Chem. Int. Ed.* 2012, **51**, 2977–2980.

[5] G. Sheldrick, *Acta Cryst.*, 2008, **A64**, 112–122.

[6] Gaussian 09, Revision D.01, M. J. Frisch, G. W. Trucks, H. B. Schlegel, G. E. Scuseria, M. A. Robb, J. R. Cheeseman, G. Scalmani, V. Barone, B. Mennucci, G. A. Petersson, H. Nakatsuji, M. Caricato, X. Li, H. P. Hratchian, A. F. Izmaylov, J. Bloino, G. Zheng, J. L. Sonnenberg, M. Hada, M. Ehara, K. Toyota, R. Fukuda, J. Hasegawa, M. Ishida, T. Nakajima, Y. Honda, O. Kitao, H. Nakai, T. Vreven, J. A. Montgomery, Jr., J. E. Peralta, F. Ogliaro, M. Bearpark, J. J. Heyd, E. Brothers, K. N. Kudin, V. N. Staroverov, T. Keith, R. Kobayashi, J. Normand, K. Raghavachari, A. Rendell, J. C. Burant, S. S. Iyengar, J. Tomasi, M. Cossi, N. Rega, J. M. Millam, M. Klene, J. E. Knox, J. B. Cross, V. Bakken, C. Adamo, J. Jaramillo, R. Gomperts, R. E. Stratmann, O. Yazyev, A. J. Austin, R. Cammi, C. Pomelli, J. W. Ochterski, R. L. Martin, K. Morokuma, V. G. Zakrzewski, G. A. Voth, P. Salvador, J. J. Dannenberg, S. Dapprich, A. D. Daniels, O. Farkas, J. B. Foresman, J. V. Ortiz, J. Cioslowski, D. J. Fox, Gaussian, Inc., Wallingford CT, 2010.

[7] a) J. P. Perdew, K. Burke, M. Ernzerhof, *Phys. Rev. Lett.* 1996, **77**, 3865–3868; b) J. P. Perdew, K. Burke, M. Ernzerhof, *Phys. Rev. Lett.* 1997, **78**, 1396; c) C. Adamo, V. Barone, *J. Chem. Phys.* 1999, **110**, 6158–6170.

[8] G. A. Petersson, A. Bennett, T. G. Tensfeldt, M. A. Al-Laham, W. A. Shirley, J. Mantzaris, *J. Chem. Phys.* 1988, **89**, 2193–2218.

[9] J. O. C. Jimenez-Halla, E. Matito, M. Solà, H. Braunschweig, C. Hörl, I. Krummenacher, J. Wahler, *Dalton Trans.* 2015, **4**, 6740–6747.

[10] T. Yanai, D. P. Tew, N. C. Handy, *Chem. Phys. Lett.* 2004, **393**, 51–57.

[11] N. M. O'Boyle, A. L. Tenderholt, K. M. Langner. *J. Comp. Chem.* 2008, **29**, 839–845.

[12] S. M. Cornet, K. B. Dillon, C. D. Entwistle, M. A. Fox, A. E. Goeta, H. P. Goodwin, T. B. Marder, A. L. Thompson, *Dalton Trans.* 2003, 4395–4405.

[13] V. N. Plakhotnik, L. Ernst, P. Sakhaii, N. F. Tovmash, R. Schmutzler, *J. Fluor. Chem.* 1999, **98**, 133–135.

[14] J. Monot, L. Fensterbank, M. Malacria, E. Lacôte, S. J. Geib, D. P. Curran, *Beilstein J. Org. Chem.* 2010, **6**, 709–712.

Cartesian coordinates of all DFT-optimised structures

1 optimised by DFT at the PBE0/6-31+G(d,p) level of theory.

Symbol	X	Y	Z
C	-4.914472	1.210286	-0.026627
C	-3.56318	1.211747	0.132673
C	-3.001568	2.629243	0.134701
C	-3.980778	3.554322	-0.056778
C	-3.859017	5.019376	0.004256
C	-4.529575	5.823868	-0.930592
C	-3.121595	5.658926	1.01423
C	-4.448562	7.212707	-0.874607
H	-5.10458	5.354275	-1.723955
C	-3.048162	7.046103	1.076416
H	-2.612495	5.057731	1.761628
C	-3.707593	7.830626	0.130351
H	-4.96813	7.812289	-1.6171
H	-2.477388	7.517659	1.871767
H	-3.649336	8.914205	0.180563
C	-1.567927	2.907284	0.33333
C	-0.858482	2.344409	1.404596
C	-0.887385	3.757744	-0.550796
C	0.487598	2.641855	1.596985
H	-1.367206	1.679196	2.096194
C	0.462317	4.038245	-0.368119
H	-1.427602	4.195357	-1.38532
C	1.153617	3.485344	0.709707
H	1.018836	2.206311	2.438584
H	0.97511	4.693135	-1.066998
H	2.206831	3.708497	0.855144
C	-2.702624	0.024358	0.279764
C	-1.558058	-0.148221	-0.512646
C	-3.026371	-0.966897	1.218198
C	-0.77308	-1.290433	-0.383919
H	-1.288474	0.611396	-1.240602
C	-2.229944	-2.098096	1.358926
H	-3.908669	-0.840106	1.838865
C	-1.103046	-2.266536	0.554522
H	0.103473	-1.41339	-1.01379
H	-2.491636	-2.852027	2.096064
H	-0.4837	-3.152686	0.66109
C	-5.798741	0.047115	-0.200386
C	-7.043573	0.003113	0.447126
C	-5.458612	-1.021178	-1.046442
C	-7.906178	-1.07636	0.276138
H	-7.329724	0.815395	1.109647
C	-6.323842	-2.094921	-1.225249
H	-4.510416	-0.998565	-1.575242
C	-7.550322	-2.130693	-0.562043
H	-8.859207	-1.091397	0.797946
H	-6.041385	-2.906007	-1.890896
H	-8.225055	-2.970309	-0.702917
B	-5.317947	2.727175	-0.173976
C	-6.774553	3.305041	-0.39788
C	-7.532177	3.850022	0.653298
C	-7.393345	3.304518	-1.660187
C	-8.813075	4.360126	0.466274
C	-8.673077	3.810046	-1.866319
C	-9.386496	4.339539	-0.798603
H	-9.365229	4.763294	1.309416
H	-9.112389	3.787168	-2.858646
C	-6.978245	3.914371	2.051394
C	-6.691768	2.732436	-2.862794
C	-10.750001	4.932219	-1.019872
F	-7.877507	3.490899	2.960953
F	-6.630476	5.162656	2.402297
F	-5.883807	3.138445	2.188813
F	-5.372477	2.567967	-2.636445
F	-7.188611	1.537408	-3.219517
F	-6.809426	3.538728	-3.935752
F	-11.395504	4.33543	-2.036487
F	-10.674579	6.244961	-1.319398
F	-11.524783	4.824234	0.073153

2 optimised by DFT at the PBE0/6-31+G(d,p) level of theory. Phenyl rings *syn*, *i.e.* in the same orientation at the crystal structure.

Symbol	X	Y	Z
B	7.927861	11.871111	0.040619
C	9.115719	12.888467	-0.27378
C	8.623416	13.61882	-1.304797
C	7.258225	13.201331	-1.728146
C	6.760082	12.169177	-1.003512
C	7.920956	10.746552	1.161774
C	7.447499	10.980636	2.466243
C	7.438544	9.995843	3.448525
H	7.057925	10.22163	4.440211
C	7.910158	8.722197	3.154301
C	8.386778	8.447432	1.879864
H	8.753031	7.454863	1.636785
C	8.38704	9.445841	0.909512
C	6.914794	12.329283	2.870187
C	7.94573	7.669666	4.226951
F	7.932379	6.428952	3.712956
F	6.897014	7.775925	5.062025
F	9.058308	7.772941	4.981742
C	8.912538	9.056712	-0.445878
C	10.439762	13.023517	0.336284
C	11.533973	13.511297	-0.403089
H	11.401177	13.756154	-1.452184
C	12.791414	13.651398	0.173116
H	13.617723	14.024202	-0.42623
C	12.997816	13.304431	1.50776
H	13.980382	13.41211	1.957975
C	11.930921	12.808637	2.254153
H	12.076056	12.531585	3.294772
C	10.673818	12.666176	1.675531
H	9.858702	12.285799	2.281323
C	9.038693	14.802788	-2.122069
H	9.661277	14.474477	-2.968273
H	9.62783	15.53259	-1.557177
C	7.695636	15.354937	-2.645716
H	7.258269	16.019199	-1.891801
H	7.805534	15.93149	-3.568546
C	6.792707	14.115034	-2.819115

H	5.721456	14.335909	-2.770073
H	6.979972	13.652828	-3.800288
C	5.469409	11.5073	-1.203342
C	4.865847	11.462093	-2.474259
H	5.384116	11.89262	-3.325364
C	3.635549	10.844512	-2.668985
H	3.198957	10.819963	-3.663856
C	2.969246	10.247995	-1.599223
H	2.008807	9.764019	-1.751054
C	3.554535	10.271877	-0.335049
H	3.048571	9.810055	0.508427
C	4.787131	10.887441	-0.142128
H	5.21608	10.900129	0.853887
F	6.963904	13.212226	1.856098
F	7.614025	12.856009	3.893361
F	5.633032	12.258277	3.276877
F	8.8979	10.092688	-1.304945
F	10.180037	8.610472	-0.378906
F	8.183739	8.069487	-0.997574

2 optimised by DFT at the PBE0/6-31+G(d,p) level of theory. Phenyl rings *anti*.

Symbol	X	Y	Z
C	-5.037213	1.166021	-0.018063
C	-3.718693	1.18328	0.288366
C	-3.153953	2.563847	0.37978
C	-4.060047	3.533686	0.106273
C	-3.833417	4.979549	0.097384
C	-4.594948	5.823338	-0.729565
C	-2.850383	5.576727	0.907361
C	-4.37449	7.196417	-0.759501
H	-5.358207	5.394587	-1.371737
C	-2.63127	6.949674	0.880305
H	-2.271444	4.9587	1.586663
C	-3.390102	7.768046	0.044428
H	-4.973696	7.822354	-1.415159
H	-1.87034	7.384815	1.522646
H	-3.22005	8.840667	0.024842
C	-5.899029	-0.00632	-0.21276
C	-7.209011	-0.02763	0.292883
C	-5.454097	-1.133651	-0.923052
C	-8.031639	-1.13628	0.115871
H	-7.579615	0.827316	0.850936
C	-6.2767	-2.240437	-1.104816
H	-4.461476	-1.125299	-1.363908
C	-7.569679	-2.249637	-0.58298
H	-9.037606	-1.129815	0.526763
H	-5.910512	-3.095855	-1.666205
H	-8.212793	-3.113194	-0.726239
B	-5.400823	2.709194	-0.132876
C	-6.848823	3.303864	-0.386709
C	-7.637716	3.833526	0.650145
C	-7.42628	3.3241	-1.667773
C	-8.911782	4.346179	0.430218
C	-8.698698	3.834608	-1.907152
C	-9.444862	4.345692	-0.853445
H	-9.490682	4.735511	1.261684
H	-9.105662	3.829888	-2.913185
C	-7.111249	3.885091	2.060241
C	-6.678985	2.766223	-2.849626
C	-10.801912	4.942745	-1.10134
F	-8.074671	3.620268	2.962286
F	-6.609604	5.092271	2.36922
F	-6.128434	2.982762	2.253327
F	-5.356045	2.682479	-2.598726
F	-7.100619	1.536034	-3.183716
F	-6.826231	3.539003	-3.942034
F	-11.382532	4.430342	-2.199241
F	-10.728083	6.277331	-1.280957
F	-11.634095	4.73413	-0.066074
C	-1.695747	2.469785	0.703985
H	-1.544039	2.626234	1.782691
H	-1.089534	3.220874	0.186489
C	-2.626076	0.203009	0.589885
H	-2.688256	-0.075904	1.652832
H	-2.676318	-0.726155	0.018366
C	-1.339926	1.015486	0.329038
H	-1.09083	0.967181	-0.73724
H	-0.478871	0.633355	0.884569

$MesBC_4Ph_4$ optimised by DFT at the PBE0/6-31+G(d,p) level of theory.

Symbol	X	Y	Z
C	-4.922694	1.220301	-0.119398
C	-3.578897	1.219438	0.096844
C	-3.024934	2.639702	0.163124
C	-4.013352	3.565049	0.023873
C	-3.884815	5.027297	0.112343
C	-4.629745	5.849719	-0.749111
C	-3.070645	5.650584	1.074437
C	-4.542672	7.237366	-0.67262
H	-5.283792	5.392321	-1.485919
C	-2.991606	7.036368	1.156863
H	-2.503337	5.03811	1.768905
C	-3.722545	7.838244	0.279793
H	-5.124233	7.849838	-1.356389
H	-2.358692	7.493242	1.913033
H	-3.659067	8.92086	0.344851
C	-1.586395	2.91049	0.344659
C	-0.863591	2.341594	1.403621
C	-0.91369	3.759123	-0.54715
C	0.487153	2.630815	1.576539
H	-1.365656	1.677274	2.10099
C	0.440245	4.032109	-0.38404
H	-1.464796	4.203854	-1.370808
C	1.144896	3.472737	0.68169
H	1.028398	2.189811	2.408967
H	0.945705	4.686861	-1.088483
H	2.201327	3.690011	0.812146
C	-2.716394	0.034865	0.266097
C	-1.559818	-0.143459	-0.507193
C	-3.050074	-0.947403	1.21042
C	-0.772815	-1.281554	-0.354153
H	-1.28186	0.60916	-1.239334
C	-2.252496	-2.074756	1.375347
H	-3.943477	-0.817737	1.814509
C	-1.11313	-2.248568	0.58993
H	0.113518	-1.40819	-0.969578

H	-2.523573	-2.821863	2.116143
H	-0.492844	-3.131662	0.715083
C	-5.794367	0.053084	-0.320273
C	-7.087133	0.041175	0.229333
C	-5.400331	-1.051414	-1.096063
C	-7.94078	-1.041953	0.036718
H	-7.423638	0.892839	0.813538
C	-6.256658	-2.128519	-1.296049
H	-4.415264	-1.056604	-1.553072
C	-7.530013	-2.133028	-0.725866
H	-8.933119	-1.028097	0.47935
H	-5.929584	-2.96772	-1.904223
H	-8.197668	-2.975669	-0.882441
B	-5.35485	2.744953	-0.182967
C	-6.789033	3.314495	-0.400913
C	-7.459638	3.986583	0.643832
C	-7.440499	3.161448	-1.64394
C	-8.749947	4.474978	0.436106
C	-8.721737	3.68393	-1.822416
C	-9.397115	4.342449	-0.793512
H	-9.262582	4.97503	1.256481
H	-9.208159	3.568094	-2.789824
C	-6.808852	4.145448	1.993147
C	-6.75108	2.465996	-2.788669
C	-10.76936	4.916345	-1.011802
H	-6.558298	3.174739	2.438816
H	-7.46881	4.667299	2.691798
H	-5.878426	4.719899	1.919745
H	-11.351321	4.924401	-0.08531
H	-11.327145	4.344971	-1.759878
H	-10.709021	5.951835	-1.368818
H	-6.51596	1.425444	-2.537542
H	-7.379302	2.459438	-3.683816
H	-5.807093	2.959015	-3.052131